Trends in Renewable Energy

Volume 1, Issue 1, March 2015

Trends in Renewable Energy

_____

Trends in Renewable Energy is a quarterly, open accessed, peer-reviewed journal publishing reviews and research papers in the field of renewable energy technology and science.

The aim of this journal is to provide a communication platform that is run exclusively by scientists working in the renewable energy field. Scope of the journal covers: Renewable energy, Catalysis for energy generation, Biofuel, Bioenergy, Biomass, Biorefinery, Biological waste treatment, Bioprocessing, Energy conservation, Energy Resources, Energy transformation, Energy storage, Environmental impact, Feedstock utilization, Future energy development, Green chemistry, Green energy, Microbial products, Physico-chemical process for Biomass, Policy, Pollution, Thermo-chemical processes for biomass, etc.

The Trends in Renewable Energy publishes the following article types: peer-reviewed reviews, mini-reviews, technical notes, short-form research papers, and original research papers.

The article processing charge (APC), also known as a publication fee, is fully waived for the initial two years for the Trends in Renewable Energy.

Editorial Team of Trends in Renewable Energy

Table of Contents

Volume 1, Issue No. 1, March 2015

Editorials

Invited Papers

Reviews

A Journal Run by Scientists

While looking for a reputable publisher to propose my own journal, Mr. Beall's blog (http://scholarlyoa.com) astonished me. An accumulated list of over 740 Predatory Publishers (Beall 2012a, Beall 2012b) contains many names, which often show up in my email box.

Is there any uncorrupted publishers? Yes, there are decent open-access publishers. Blue chip companies hosting hundreds of journals which charge $2000-5000 per accepted manuscript. Few small publishers charge a reasonable amount of money, but only can host less than ten journals due to limited sources.

Can scientists operate our own journal? We surely can. We are trained to be able to learn anything. This kind of successful stories is rare, but always inspiring us. By launching this journal, I want to show our scientific attitudes.

Our Scientific Attitudes

A scientific journal should be run by scholars, scientists, researchers, and engineers. Since we are not businessmen, we mind scientific values.

Making a good journal is the most important thing. I have seen that a SCI journal decreased its impact factor from 1.5 to 0.3 within 5 years, and understood how hard to maintain a reputable publication. The goal of this journal is to pass EI Compendex review within 5 years, and be included in SCI index within 7 years.

In order to make a good journal and achieve these goals, it needs the collaborative effort among our editorial board members, authors, reviewers, and all contributors.

We show respect for scholars. The first two volumes of the journal are free of any charge to authors. The length of this Article Processing Charge (APC) waive period may be extended, if the editorial board thought it's necessary.

We show respect to our editors, editorial board members, and reviewers. After the APC waive period, we will waive APC for manuscripts submitted by our editorial team, and provide 50% discount to reviewers.

This Journal

Trends in Renewable Energy (U.S. ISSN: 2376-2136, online ISSN: 2376-2144) is a peer-reviewed open access journal that is run exclusively by scientists. It aims to provide a fair platform among scholars, and share our knowledge in the energy related areas. Scope of the journal covers: Renewable energy, Catalysis for energy generation, Biofuel, Bioenergy, Biomass, Biorefinery, Biological waste treatment, Bioprocessing, Energy conservation, Energy Resources, Energy transformation, Energy storage, Environmental impact, Feedstock utilization, Future energy development, Green chemistry, Green energy, Microbial products, Physico-chemical process for biomass, Policy, Pollution, Thermo-chemical processes for biomass, etc. We publish the following article types: reviews, mini-reviews, technical notes, short-form original research papers, and research papers.

Bo Zhang
Editor in Chief

REFERENCES

Beall, J. (2012a). "Predatory publishers are corrupting open access." *Nature*, 489, 179.
   DOI: 10.1038/489179a

Beall, J. (2012b). "Criteria for determining predatory open."
   http://scholarlyoa.com/2012/11/30/criteria-for-determining-predatory-open-access-publishers-2nd-edition/. [Accessed on October 3, 2014]

Renewable Energy for a Sustainable Future

Dear colleagues,

It is with great pleasure that we present to you our new international open accessed journal in the field of renewable energy. Renewable energy is a comprehensive and interdisciplinary area, which covers Chemistry, Biology, Chemical Engineering, Mechanic Engineering, Material Science, Economic, Environmental Science, Agricultural Engineering, etc. And this journal would be a prodigious platform for all scientists and engineers working dedicatedly in this field.

Though coal remains as the dominate energy source in China, renewable energy has tremendous growth over the last 15 years. Currently, China was the main demand driver, accounting for more than 80% of the global market. By the end of 2013, China, the United States, Brazil, Canada, and Germany remained the top countries for total installed renewable power capacity; the top countries for non-hydro capacity were again China, the United States, and Germany, followed by Spain, Italy, and India (REN21 2014). China's new renewable power capacity surpassed new fossil fuel and nuclear capacity for the first time. China lead the world in the production and use of wind power, solar photovoltaic cells, and smart grid technologies, generating almost as much hydro-, wind and solar power as all of France and Germany's power plants combined (Mathews and Tan 2014).

Scientists at the Wuhan Institute of Technology are dedicated to renewable energy researches, including high-value chemicals production from cellulosic biomass, bioseparation technologies, bioprocessing of microalgae, and CO_2 capture. We look forward to sharing our progress with all colleagues through this platform.

Congratulations on the launch of Trends in Renewable Energy and best wishes for the success of the journal.

Changyan Yang, Ph.D.
Professor and Vice Dean for Research
School of Chemical Engineering & Pharmacy
Wuhan Institute of Technology

REFERENCES

REN21 (2014). "Renewables 2014 Global Status Report."
http://www.ren21.net/portals/0/documents/resources/gsr/2014/gsr2014_full%20report_low%20res.pdf. [Accessed on 2/17/2015]
Mathews, J. A. and Tan, H. (2014). "Economics: Manufacture renewables to build energy security." *Nature*, 513, 166–168, DOI: 10.1038/513166a.

Development of Green Biorefinery for Biomass Utilization: A Review

Shuangning Xiu[*] and Abolghasem Shahbazi

Department of Natural Resources and Environmental Design, North Carolina A&T State University, Greensboro, North Carolina, 27411 USA

Green biorefineries are multiproduct systems, which utilize green biomass as an abundant and versatile raw material for the manufacture of industrial products. It represents an innovative approach to alternative applications of surplus grassland biomass. An overview of the main aspects, activities, and processing technologies was presented in this paper. Recent developments on the green biorefinery in both Europe and North America were discussed. A focus for future R&D work in this field was recommended.

Introduction

Non-renewable fossil fuels, coal, oil and natural gas are being consumed worldwide at a very fast pace (Shafiee and Topal 2009). The United States consumes more than 25% of international oil production, but possesses just 1.6% of its oil reserves (US EPA 2009). If not replaced by alternative energy sources, fossil fuels will eventually be depleted while CO_2 in the atmosphere will rise to levels with dangerous consequences. Fossil fuels are the major source of environmental pollutants, greenhouse gases, and ocean acidification. Sustainable development requires the use of renewable resources as alternative feedstocks for chemical, fuel and material production.

Biomass represents an attractive source for the production of fuels and chemicals due to its versatility, renewable nature, and low environmental impacts. Considerable attention has been given to lignocellulosic biomass such as agricultural residues and energy crops for biofuel production. US Department of Energy (DOE) and Department of Agriculture (USDA) projected that the US biomass resources could provide approximately 1.3 billion dry tonnes of feedstock for biofuels, which would meet about 40% of the annual US fuel demand for transportation (Perlack *et al.* 2005). The overall goal is to replace 20% of the United States transportation fuel imports (35 billion barrels per year) by 2017 (Biomass Research and Development Board 2008). Obviously, a significant need exists for exploring its efficient utilization.

There has been an increasing interest in the use of perennial grasses as energy crops in the US and Europe since the mid-1980s. Over time, various conversion technologies have been used to produce biofuels from perennial grasses. Conversion technologies can be subdivided into two categories: thermochemical treatment (*e.g.*, pyrolysis, gasification, hydrothermal liquefaction, and combustion) and biological treatment (*e.g.*, fermentation, anaerobic digestion). Water contained in green biomass

poses the negative effect on the thermochemical treatment, as it requires the high heat of vaporization. In general, drying the "nature-wet" raw material is needed for the thermochemical conversion technologies, which limits the options for green biomass as feedstock and overall process economy.

Researchers also found that biomass from semi-natural grasslands is difficult to exploit in conventional bioenergy-converting systems, as the chemical composition is detrimental for both conventional anaerobic digestion as a result of high fiber concentrations (Prochnow *et al.* 2005, Richter *et al.* 2009) and for cellulosic bioethanol fermentation due to its resistance to enzymatic attack. Cellulosic biomass must be pretreated before it can be enzymatically hydrolyzed.

Despite advances in technology, the ability to produce biofuel as a single source of revenue remains infeasible (US EPA 2007) and exhibits a need for further cost reductions. One possibility for ameliorating this problem is to adopt a biorefinery approach which diversifies the output streams of a biofuel facility by generating diverse co-products alongside biofuel for increased revenue generation (Takara and Khanal 2011).

Analogous to the petroleum refinery that processes a barrel of crude oil into many petroleum based products including gasoline, diesel fuels and petroleum based chemicals, the biorefinery converts biomass into multiple biofuels and bioproducts. The ability to process raw materials into a varied product stream greatly enhances the versatility of the biorefinery to meet the economic demands of the free market and compete globally. This pioneering concept has been examined for several feedstocks, including alfalfa and Bermuda grass for biofuel and protein recovery applications (Buentello *et al.* 1997, Dale and Matsuoka 1981, Dale 1983).

The technological concept of green biorefinery represents an innovative approach to alternative applications of green biomass. This article comprehensively reviewed the state of the art, the feedstocks, and the processing technologies that are used to produce multiproduct in the green biorefinery. Besides, the research development status in both Europe and North America were discussed. It also recommended future R&D work in the green biorefinery field.

Green Biorefinery

Concept of Green Biorefinery

Green biorefineries are multiproduct systems, which utilize green biomass as an abundant and versatile raw material for the manufacture of industrial products. The concept is currently in an advanced stage of development in several European countries, especially Germany, Denmark, Switzerland, the Netherlands and Austria (Xiu and Shahbazi 2013).

The basic idea of this concept is to utilize the whole green biomass (like grass, alfalfa, and various other sources) to generate a variety of products that are either valuable products themselves or form the basis for further production lines. Besides biobased materials, fuels and energy may be supplied by this technology. The feasibility of a biorefinery based on grass has been successfully demonstrated by (Grass and Hansen 1999).

In green biorefinery, the careful wet or green fractionation technology is used as the first step (primary refinery) to isolate the green biomass substances in their natural form. Thus, green biomass are separated into a fiber-rich press cake and a nutrient-rich

press juice (Figure1). Both fractions have an economic value. Figure1 illustrates the array of potential products from a green biorefinery that can be generated by the downstream processing of press juice and press cake.
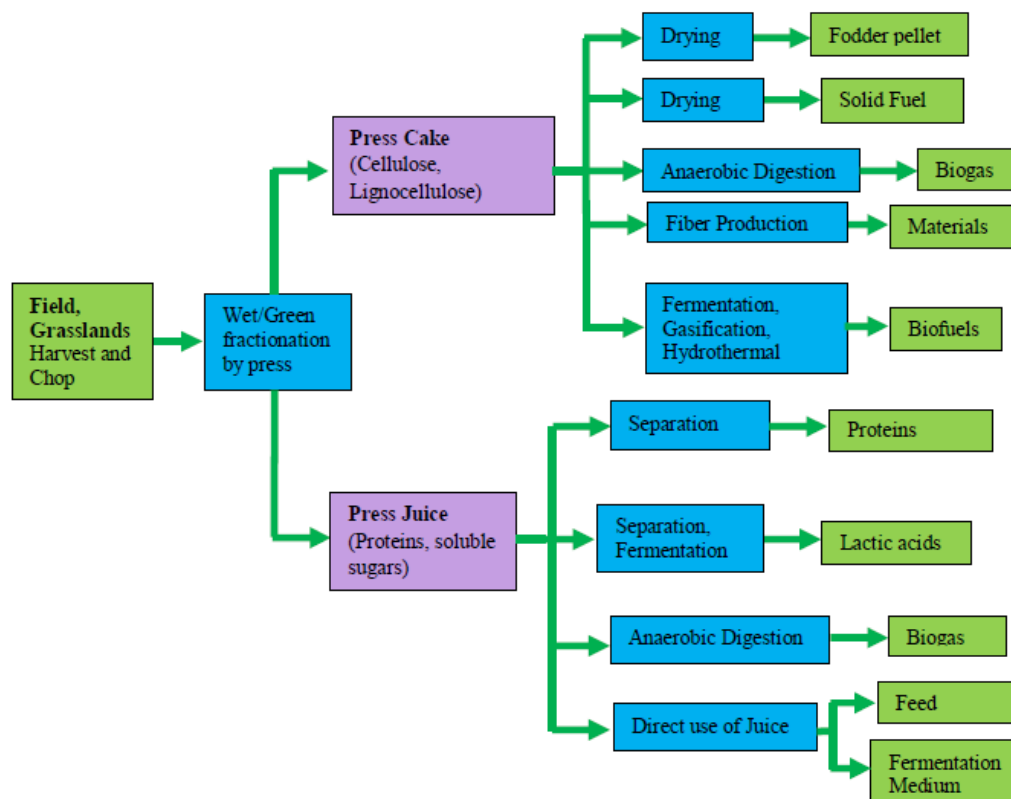
Figure 1. A green biorefinery system for green biomass utilization.

Feedstocks for Green Biorefinery

Currently, the feedstocks used for green biorefinery are mainly green grasses, for example, grass from cultivation of permanent grass lands, closure fields, nature preserves, or green crops such as Lucerne (or Alfalfa), clover, and immature cereals from extensive land cultivation (Kamm and Kamm 2007). The interesting valuable components of fresh biomass are proteins, soluble sugars, and the fiber fractions (*i.e.* cellulose, hemicelluloses, and lignin parts).

Table 1 shows the chemical composition of representative types of green biomass. In general, biomass are typically composed of 75-90% of sugar polymers, with the other 10-25% of biomass principally being lignin (Huber and Dumesic 2006). For herbaceous grass plants, typical contents in the dry mater are in the range of 6-15% for protein, 20-55% water soluble extracts containing 5-16% soluble sugars and the raw fiber parts (cellulose 20-30%, hemicelluloses 15-25%, and lignin 3-10%) (Mandl 2010).

In the past, most of attention has focused on the cellulose, hemicelluloses, and lignin existing in cellulosic materials. However, there are also considerable amounts of protein available in these biological materials as indicated in Table 1. For the biomass species listed, aquatic organisms, especially algal species, often have higher protein content than other biomass resources. For example, *Spirulina* algae have a high protein content of around 60%. Since a kilogram of protein is generally much more valuable than

an equal weight of carbohydrate, aquatic organisms can be used as a good candidate for green biorefinery in respect of high value protein recovery.

Nowadays, algae are viewed as next generation biofuel feedstocks because of their superior photosynthetic efficiencies and higher carbon capturing capabilities compared with terrestrial plants (Hasan *et al.* 2013). Algae are usually composed of lipids, proteins, nucleic acids, and no-cellulosic carbohydrates. Conversional algae-to-biodiesel technology requires drying of the algal biomass followed by solvent and or/mechanical extraction. The energy consumed in drying process is more than 75% of the total energy consumption (Lardon *et al.* 2009). In the green refinery, the wet fractionation of algae can be employed to reduce the need for energy-intensive drying operations and to utilize nutrient-rich green juice for value-added co-product developments (*e.g.*, protein) that would otherwise be destroyed in downstream processing.

Besides algae, energy crops such as switchgrass and grant miscanthus can be good candidates for green biorefinery due to the high yields of biomass per hectare and year, low fertilization and pesticide requirements, broad adaptability, and greater ability to sequester carbon in the oil than most other grasses. Switchgrass (*Panicum virgatum L.*) is a perennial native grass adapted to the prairies of North America, and was identified by the DOE as a primary species for development as an energy crop. It has the ability to grow well on marginal croplands without heavy fertilization or intensive managements and has a potential for the high fuel yield (Woodward 2008).

Table 1. Composition of representative biomass resources

Biomass type	Aquatic organisms		Herbaceous		Woody	
Name	*Spirulina*	Duckweed	Bermuda grass	Switch grass	Poplar	Pine
Component (dry wt%)						
Celluloses	<1	11.9	31.7	37	41.3	40.4
Hemicellulose	1	13.8	40.2	29	32.9	24.9
Lignin	<1	3.2	4.1	19	25.5	34.5
Crude protein	64	35.1	12.3	3	1.7	0.7
Crude lipid	5	5	11.9	--	--	--
Ash	11	16.5	5	6	0.8	0.5
Total	100	92.4	93.3	94	102.9	101.0
Reference	(Vardon *et al.* 2012)	(Xiu *et al.* 2010)	(Huber and Dumesic 2006)	(US Department of Energy)	(Huber and Dumesic 2006)	(Huber and Dumesic 2006)

Grant Miscanthus (*Miscanthus x giganteus*) is a tall perennial grass that reproduces by underground rhizomes and has been evaluated in Europe during the past 10 years as a bioenergy crop. It is characterized as having broad adaptability, high water and fertilizer use efficiency, excellent pest resistance, and tremendous biomass production. Tonnages of between 6-20 tonnes/acre are anticipated from miscanthus. Miscanthus stems may be used as fuel for the production of heat and electric power or as a feedstock for the production of cellulosic ethanol. In general, the advantages of using energy crop as feedstock is its high biomass profit per hectare and a good coupling with national and state's priority to use energy crops as second generation biofuel feedstock.

Current Processing Technologies for Green Biorefinery

Primary Separation

The initial fractionation of the green biomass remains an essential operation for green biorefinery process. Green crop fractionation is now studied in about 80 countries (Singh 1996). Water contents in tropical grasses can be as high as 80-85% or similarly ~90% for aquatic species. Those "nature-wet" raw materials require a fast primary processing or the use of preservation methods, like silage or drying. But due to the energy consumption of thermal dryers, the biomass is seldom transformed after drying, so that mechanical fractionation of the wet material is usually the first unit operation in the green biorefinery plant. Screw press machine has been primarily used to press the green juice out of the green biomass. For vegetative biomass like alfalfa, clover and grass, screw presses remove approximately 55-60% of the inherent liquid (Kamm *et al.* 2009). Nevertheless other means of preprocessing have also been applied, such as thermal mechanical dewatering method, simultaneous application of a pulsed electric field, and superimposition of ultrasounds (Arlabosse *et al.* 2011). Wachendorf *et al.* investigated the hydrothermal conditioning at different temperatures (5, 60 and 80°C) and mechanical dehydration on mass flows of plant compounds into the press fluid for five grassland pastures typical of mountain areas of Germany. The underlying objectives were to obtain a juice in larger quantity and of better quality (Wachendorf *et al.* 2009).

Processing of Press Juice to Value-added Products

The green juice contains proteins, free amino acids, organic acids, dyes, enzymes, hormones, other organic substances, and minerals (Kamm and Kamm 2007). The green juice is a good source for high quality fodder proteins, cosmetic proteins, human nutrition or platform chemicals like lactic acid and lysine or can be used as substrate for bio-gas production (Kamm *et al.* 2009). The main focus is to process the juice into products such as lactic acid and corresponding derivatives, amino acids, ethanol, and proteins.

The best known products which can be obtained from grassland biomass are proteins. Proteins are essential elements of the nutrition for humans and animals, and important raw materials for adhesives and for the pharmaceutical and cosmetics industries. Protein extraction from fresh alfalfa have been explored since 80s' (Dale and Matsuoka 1981, Dale 1983, Pirie 1986).

High-quality fodder proteins and proteins for cosmetic industry may be produced through the fractionation of the green juice proteins in different separation and drying processes. The fodder proteins could be a complete substitute for soy proteins. They even have a nutritionally physiologic advantage due to their special amino acid patterns. The general approach to leaf protein production is to harvest fresh plant materials, grind the plant tissue, squeeze out a protein rich juice and then heat the juice to precipitate and recover the protein (Pirie 1971).

Recently, L-lactic acid received increased attention as a feedstock monomer for a biodegradable polymer-polylactide (PLA). A recent study has demonstrated that, after separation of proteins from alfalfa press juice, the supernatant can be used as fermentation media for the production of the ammonium lactate, L-lysine-L-Lactate, which acts as intermediates for the production of lactic acid sequence products like lactide (Leiß *et al.* 2010). Another study evaluated the possibility of recovery of lactic acid from various grass silages through a two-step process, in which the crude liquid press extract was pre-treated with ultrafiltration membranes followed by purification with

mono-polar electrodialysis (Danner *et al.* 2000). Lactic acid can also be separated from grass silage juice by chromatography using neutral polymeric resin (Thang and Novalin 2008).

Alternatively, press juice can be directly used as fermentation media for organic acids production. When the fermentation experiments of lactic acid bacteria were carried out in brown juice, the result showed that juices from grass, clover and alfalfa can easily be converted to a stable universal fermentation media by adding more carbohydrates or for production of other organic acids or amino acids in the second stage fermentation (Anderson and Kiel 2000). This is a new way of simultaneous preservation and utilization of plant juice for fermentation purposes.

Processing of Press Cake to Value-added Products

The press cake can be used as solid fuels, for the production of green feed pellets/fodder pellets, as a raw material for the production of chemicals, such as levulinic acid, and for the conversion to syngas and hydrocarbons (synthetic biofuels).

Richter *et al.* evaluated the properties of the press cakes as solid fuel, which was derived from five species-rich, semi-natural grasslands via thermal mechanical dewatering method (Richter *et al.* 2009). Their results showed that compared with the grassland silages used as parent materials, the press cakes generated significantly lower concentrations of elements detrimental for combustion. The ash softening temperature of the press cakes increased significantly, which was comparable to beech wood. Overall, the solid fuel from press cakes was of superior quality compared with conventional hay. However, the increase in the higher heating value of these press cakes was not statistically significant.

Other uses of the press cakes include manufacturing fodder pellets and biogas production. The residues of green biorefinery are suitable for the production of biogas, combined with the generation of heat and electricity. In Europe, the green crop drying industry produces fodder pellets by drying crops such as perennial ryegrass, Italian ryegrass, clover grass and alfalfa (Thomsen 2005, Walker *et al.* 1982). From an energetic point of view, it is far better to use the press cake as a silage feed and/or bioenergy.

Since the press cake is rich in fiber, researchers have commented on the potential use of press cake for fiber applications (*e.g.*, insulation materials, fiber boards, horticultural substrates, and pulp & paper) (Mandl 2010). However, little or no attention has been devoted to removing and upgrading the carbohydrate fraction of press cake for fiber applications. Therefore, there is a need to develop and demonstrate technologies for utilizing green biomass for various fiber applications.

Biomass conversion to fuels and chemicals is receiving a great deal of attention. The need for a billion tonnes of biomass to produce enough biofuel to replace 30% of US petroleum consumption has been reported by the US DOE (Woodward 2008). The integrated green biorefinery system will certainly enhance the economics of biofuel production by generating value-added co-products from biomass. The research contributed to this effort has been primarily focused on protein recovery in bioethanol production (Dale 1983, Kammes *et al.* 2011, Takara and Khanal 2011).

Besides fuel ethanol production, other biofuels and chemicals can be produced from press cake as well. The thermochemical conversion process is another promising method of converting the press cake for energy purposes. For instance, the syngas produced from grassed may be converted to fuel alcohols via the Fischer-Tropsch process (Boateng *et al.* 2006).

Research Development Status in Green Biorefinery

Research Status in Europe

The most notable successes in research and development in the field of green biorefinery system research happened in several European countries. The pilot scale processing trials in Austria (Utzenaich), Denmark (Esbjerg), Switzerland (Obre), and Germany (Brandenburg) have produced lactic acid, amino acids, leaf juice protein concentrate, fiber products, and biogas by setting up integrated refineries (Mandl 2010). In 2001, the first Green Biorefinery started operation in Switzerland with a design load of 5000 tonnes dry matter of grass per year and a combined output of fibers (0.4 tonnes per ton input), protein (160 t/t), and bioenergy (500kWh/t) (Baier and Grass 2001). A green biorefinery demonstration plant in Havelland (Germany) is under construction, which will have an annual capacity of 20,000 tonnes alfalfa and grass biomass and can be diversified in modules for the production of platform chemicals and synthesis gas. The demonstration facility will directly link to the existing green crop drying plants (Kamm *et al.* 2010).

Since 1999, Dr. Kromus's research group in Australia has started to develop the Austrian green biorefinery and the results lead to the installation of a basic pilot plant in 2004 (Kromus *et al.* 2004). A key element in their concept is the utilization of fermented grass (*i.e.* grass silage) instead of fresh biomass.

However, the majority of the biorefineries in Europe are based on wet fractionation process to isolate the substrate fractions in their natural form (*i.e.* pressed fiber and nutrient-rich juice from fresh grass or silage) and to develop platform chemicals from the green/brown juice. The press cake has been primarily used for production of fodder pellet and biogas. Little or no attention has yet been focused on the utilization of the press fiber for fuel purpose, especially as raw materials for biofuel production.

Research Status in North America

The research development in green biorefinery in North American is not as significant as that in Europe. The research has being primarily focused on protein recovery in ethanol production. Various groups in North American have been examining various grasses for their potential as feedstocks for biofuel production. Haque *et al.* in Oklahoma evaluated productivity of four grasses (Bermuda, faccid, love and switch) and reported that switchgrass is the most viable species for biofuel production (Haque *et al.* 2009). Woodward evaluated the potential for alfalfa, switchgrass, and miscanthus as biofuel corps in Washington State (Woodward 2008). Research group in Nebraska also found that switchgrass-derived ethanol produced 540% more energy than was required to manufacture the fuel. One acre of grassland could, on average, delivers 320 gallons of bioethanol (Schmer *et al.* 2008). Another research group in Hawaii has developed an innovative biorefinery approach to green processing of tropical banagrass into biofuel and biobased products (Bals *et al.* 2007). Edwards *et al.* has extracted leaf protein form orchard grass and switchgrass, which is indented to use as a source of protein for livestock (Edwards *et al.* 1975).

Future R&D Work

Table 2 summarized various green biorefinery developments through the world. The most promising products which have been identified from the green juice are 1) proteins: as feed or food (low price), hydrolyzed as amino acids for cosmetics or

pharmaceutical industry, and 2) lactic acid: for neutralization/buffering, as solvent (ethyl lactate), or bioplastics (PLA=polylactide).

Table 2. Green biorefinery of different green biomass in literature

Grass Type	Main products		Country	Reference
	Press Juice	Press Cake		
Alfalfa, mixed grass	Protein, fermentation media	Animal feed, biogas	Germany	(Kamm *et al.* 2010, Richter *et al.* 2009)
Grass silage (red clover and ryegrass)	Protein Lactic acid	Fibers	Austria	(Danner *et al.* 2000)
Alfalfa	Protein	Ethanol	US	(Dale 1983)
Tropical banagrass	Edible fungus for aquaculture feed supplement	Ethanol	US	(Takara and Khanal 2011)
Orchard grass and switchgrass	Protein as animal feed	Ethanol	US	(Kammes *et al.* 2011)
Grass, clover and alfalfa	Fermentation media	Fodder pellets for animal feed	Denmark	(Anderson and Kiel 2000)
Silage	Protein as animal feed	Fiber, biogas	Switzerland	(Baier and Grass 2001)
Switch grass	Protein	n/a	US	(Bals *et al.* 2007)

To date, the economic viability of green biomass fractionation press, for instance the ProXan-Process (Edwards *et al.* 1975) used to produce a marketed leaf protein concentrate, depends, to a large extent, on the utilization of the solid fraction as high quality ruminant feed (Sinclair 2009). The production of only one product such as, for example, a protein product would not create sufficient revenue to cover the cost of the raw material and the related processing costs.

In the area of the press cake utilization, the research interest is directed to fodder pellets and biogas production in Europe and ethanol production in US, respectively. The alternative use of grass press cake as a potential raw material for second-generation biofuels has not been worked on in detail so far, but it is indeed worthwhile exploring. Co-generation of biofuels from the green biorefinery would certainly "upgrade" the green biorefinery approach in the minds of strategists and decision-makers. Besides biofuels, the press cake could also be feedstock for generation of bioproducts, such as lactic acid, which is a base chemical for many applications, from food additive to solvents to plastics. Therefore, there is a need to develop and evaluate the state-of-art biomass conversion technologies for generating biofuels and bioproducts from grass press cake.

CONCLUSIONS

A green biorefinery offers a solution to generate a variety of products and energy without directly interfering in the food supply chain by utilizing surplus resources. Some R&D work has been done over the last 15 years and technologies have been pushed forward to demonstration plants in several European countries. However, there is no real impact from an industrial perspective so far. Some problems affecting its industrial utilization and recommendations are described as follows:

1   Feedstock selection and evaluation. Currently, the feedstocks used for green biorefinery are mainly green grass and/or green crops. Better management of species and varieties including the use of second generation biofuel feedstocks (*e.g.*, microalgae) could reduce the associated carbon footprint and improve the production efficiency of the green biorefinery.

2   The development of technologies for the production of biofuels and bioproducts from the press cake. In the area of the press cake utilization, the research interest is directed to fodder pellets and biogas production in Europe and ethanol production in US, respectively. Little attention has been devoted to the alternative use of press cake as a raw material for second-generation biofuels and bioproducts production. Therefore, there is a growing demand for developing and evaluating the state-of-art biomass conversion technologies for generating biofuels and bioproducts from grass press cake. Thus, the overall economic efficiency of a green biorefinery will improve.

3   Development of industrial green biorefinery technologies. Over the years, different green biorefinery schemes have been proposed and investigated. However, none of them has been commercialized yet. Research should focus on the further development of alternative products and pave the way for the implementation of a green biorefinery.

4   Evaluation of the overall sustainability of process technologies. Research should evaluate these aspects of sustainability considering costs and emissions involved with input production, feedstock production, feedstock harvest, transport, storage, pre-processing, processing, product transportation, and consumption.

ACKNOWLEDGMENTS

CONFLICTS OF INTEREST

The authors declare that there is no conflict of interests regarding the publication of this paper.

REFERENCES

Anderson, M., and Kiel, P. (2000). "Integrated utilization of green biomass in the green biorefinery." *Industrial Crops and Products*, 11, 129-137. DOI: 10.1016/S0926-6690(99)00055-2

Arlabosse, P., Blanc, M., Kerfaï, S., and Fernandez, A. (2011). "Production of green juice with an intensive thermo-mechanical fractionation process. Part I: Effects of processing conditions on the dewatering kinetics." *Chemical Engineering Journal*, 168(2), 586-592. DOI: 10.1016/j.cej.2011.01.027

Baier, U., and Grass, S. (2001). "Bioraffination of Grass, Anaerobic Digestion 2001." *Proceedings of the 9th World Congress for Anaerobic Conversion for Sustainability,* Antwerpen.

Bals, B., Teachworth, L., Dale, B., and Balan, V. (2007). "Extraction of Proteins from Switchgrass Using Aqueous Ammonia within an Integrated Biorefinery." *Applied*

Biochemistry and Biotechnology, 143(2), 187-198. DOI: 10.1007/s12010-007-0045-0

Biomass Research and Development Board (2008). "National Biofuels Action Plan." *http://www1.eere.energy.gov/biomass/pdfs/nbap.pdf*. [Accessed on February 20, 2015]

Boateng, A. A., Jung, H. G., and Adler, P. R. (2006). "Pyrolysis of energy crops including alfalfa stems, reed canarygrass, and eastern gamagrass." *Fuel*, 85(17–18), 2450-2457. DOI: 10.1016/j.fuel.2006.04.025

Buentello, J. A., Gatlin, D. M., and Dale, B. E. (1997). "Evaluation of Coastal Bermuda Grass Protein Isolate as a Substitute for Fishmeal in Practical Diets for Channel Catfish Ictalurus punctatus." *Journal of the World Aquaculture Society*, 28(1), 52-61. DOI: 10.1111/j.1749-7345.1997.tb00961.x

Dale, B. E., and Matsuoka, M. (1981). "Protein recovery from leafy crop residues during biomass refining." *Biotechnology and Bioengineering*, 23(6), 1417-1420. DOI: 10.1002/bit.260230624

Dale, B. E. (1983). "Biomass refining: protein and ethanol from alfalfa." *Industrial & Engineering Chemistry Product Research and Development*, 22(3), 466-472. DOI: 10.1021/i300011a016

Danner, H., Madzingaidzo, L., Holzer, M., Mayrhuber, L., and Braun, R. (2000). "Extraction and purification of lactic acid from silages." *Bioresource Technology*, 75(3), 181-187. DOI: 10.1016/S0960-8524(00)00068-7

Edwards, R. H., Miller, R. E., De Fremery, D., Knuckles, B. E., Bickoff, E. M., and Kohler, G. O. (1975). "Pilot plant production of an edible white fraction leaf protein concentrate from alfalfa." *Journal of Agricultural and Food Chemistry*, 23(4), 620-626. DOI: 10.1021/jf60200a046

Grass, S., and Hansen, G. (1999). "Production of ethanol and biogas, protein concentrate and technical fibers from grass/clover."In: *Biomass Congress of the Americas, Proceedings; Oakland, USA*.

Haque, M., Epplin, F. M., and Taliaferro, C. M. (2009). "Nitrogen and Harvest Frequency Effect on Yield and Cost for Four Perennial Grasses All rights reserved. No part of this periodical may be reproduced or transmitted in any form or by any means, electronic or mechanical, including photocopying, recording, or any information storage and retrieval system, without permission in writing from the publisher." *Agron. J.*, 101(6), 1463-1469. DOI: 10.2134/agronj2009.0193

Hasan, R., Zhang, B., and Wang, L. (2013). "Microalgae for Biodiesel Production and Waste Water Treatment."In: *Biomass Processing, Conversion and Biorefinery*, B. Zhang, and Y. Wang, eds., Nova Science Publishers, Inc., Hauppauge NY, 277-288.

Huber, G. W., and Dumesic, J. A. (2006). "An overview of aqueous-phase catalytic processes for production of hydrogen and alkanes in a biorefinery." *Catalysis Today*, 111(1–2), 119-132. DOI: 10.1016/j.cattod.2005.10.010

Kamm, B., and Kamm, M. (2007). "International biorefinery systems." *Pure Appl.Chem.*, 79(11), 1983-1997.

Kamm, B., Schönicke, P., and Kamm, M. (2009). "Biorefining of green biomass – technical an energetic considerations." *CLEAN – Soil, Air, Water*, 37, 27-30.

Kamm, B., Hille, C., Schönicke, P., and Dautzenberg, G. (2010). "Green biorefinery demonstration plant in Havelland (Germany)." *Biofuels, Bioproducts and Biorefining*, 4(3), 253-262. DOI: 10.1002/bbb.218

Kammes, K. L., Bals, B. D., Dale, B. E., and Allen, M. S. (2011). "Grass leaf protein, a coproduct of cellulosic ethanol production, as a source of protein for livestock." *Animal Feed Science and Technology*, 164(1–2), 79-88. DOI: 10.1016/j.anifeedsci.2010.12.006

Kromus, S., Wachter, B., Koschuh, W., Mandl, M., Krotscheck, C., and Narodoslawsky, M. (2004). " The green biorefinery Austria – development of an integrated system for green biomass utilization." *Chemical and Biochemical Engineering Quarterly*, 18, 7–12.

Lardon, L., Hélias, A., Sialve, B., Steyer, J.-P., and Bernard, O. (2009). "Life-Cycle Assessment of Biodiesel Production from Microalgae." *Environmental Science & Technology*, 43(17), 6475-6481. DOI: 10.1021/es900705j

Leiß, S., Venus, J., and Kamm, B. (2010). "Fermentative Production of L-Lysine-L-lactate with Fractionated Press Juices from the Green Biorefinery." *Chemical Engineering & Technology*, 33(12), 2102-2105.

Mandl, M. G. (2010). "Status of green biorefining in Europe." *Biofuels, Bioproducts and Biorefining*, 4(3), 268-274. DOI: 10.1002/bbb.219

Perlack, R. D., Wright, L. L., Turhollow, A. F., Graham, R. L., Stokes, B. J., and Erbach, D. C. (2005). "Biomass as feedstock for a bioenergy and bioproducts industry: The technical feasibility of a billion-ton annual supply." *http://www1.eere.energy.gov/bioenergy/pdfs/final_billionton_vision_report2.pdf*. [Accessed on February 20, 2015]

Pirie, N. W. (1971). *Leaf protein: its agronomy, preparation, quality and use*, International Biological Programme.

Pirie, N. W. (1986). "Leaf protein after forty years." *BioEssays*, 5(4), 174-175. DOI: 10.1002/bies.950050409

Prochnow, A., Heiermann, M., Drenckhan, A., and Schelle, H. (2005). "Seasonal Pattern of Biomethanisation of Grass from Landscape Management." *Agricultural Engineering International: CIGR Journal*, 7, Manuscript EE 05 011.

Richter, F., Graß, R., Fricke, T., Zerr, W., and Wachendorf, M. (2009). "Utilization of semi-natural grassland through integrated generation of solid fuel and biogas from biomass. II. Effects of hydrothermal conditioning and mechanical dehydration on anaerobic digestion of press fluids." *Grass and Forage Science*, 64(4), 354-363. DOI: 10.1111/j.1365-2494.2009.00700.x

Schmer, M. R., Vogel, K. P., Mitchell, R. B., and Perrin, R. K. (2008). "Net energy of cellulosic ethanol from switchgrass." *Proceedings of the National Academy of Sciences*, 105(2), 464-469. DOI: 10.1073/pnas.0704767105

Shafiee, S., and Topal, E. (2009). "When will fossil fuel reserves be diminished?" *Energy Policy*, 37(1), 181-189. DOI: 10.1016/j.enpol.2008.08.016

Sinclair, S. (2009). "Protein extraction from pasture. Literature review Part A: The plant fractionation bio-porcess and adaptability to farming systems." *http://maxa.maf.govt.nz/sff/about-projects/search/C08-001/literature-review.pdf*. [Accessed on February 20, 2015]

Singh, N. (1996). *Green Vegetation Fractionation Technology*, Science Publishers, Inc., Lebanon, NH, USA.

Takara, D., and Khanal, S. K. (2011). "Green processing of tropical banagrass into biofuel and biobased products: An innovative biorefinery approach." *Bioresource Technology*, 102(2), 1587-1592. DOI: 10.1016/j.biortech.2010.08.106

Thang, V. H., and Novalin, S. (2008). "Green Biorefinery: Separation of lactic acid from grass silage juice by chromatography using neutral polymeric resin." *Bioresource Technology*, 99(10), 4368-4379. DOI: 10.1016/j.biortech.2007.08.045

Thomsen, M. (2005). "Complex media from processing of agricultural crops for microbial fermentation." *Applied Microbiology and Biotechnology*, 68(5), 598-606. DOI: 10.1007/s00253-005-0056-0

US Department of Energy "Biomass Feedstock Composition and Property Database." *http://www.afdc.energy.gov/biomass/progs/search1.cgi*. [Accessed on February 20, 2015]

US EPA (2007). "Biofuels in the U.S. Transportation Sector." *http://www.eia.gov/oiaf/analysispaper/biomass.html*. [Accessed on February 20, 2015]

US EPA (2009). "U.S. Crude Oil, Natural Gas, and Natural Gas Liquids Reserves 2007 Annual Report." *http://www.eia.gov/naturalgas/crudeoilreserves/archive/2007/full.pdf*. [Accessed on February 20, 2015]

Vardon, D. R., Sharma, B. K., Blazina, G. V., Rajagopalan, K., and Strathmann, T. J. (2012). "Thermochemical conversion of raw and defatted algal biomass via hydrothermal liquefaction and slow pyrolysis." *Bioresource Technology*, 109(0), 178-187. DOI: 10.1016/j.biortech.2012.01.008

Wachendorf, M., Richter, F., Fricke, T., Graß, R., and Neff, R. (2009). "Utilization of semi-natural grassland through integrated generation of solid fuel and biogas from biomass. I. Effects of hydrothermal conditioning and mechanical dehydration on mass flows of organic and mineral plant compounds, and nutrient balances." *Grass and Forage Science*, 64(2), 132-143. DOI: 10.1111/j.1365-2494.2009.00677.x

Walker, H. G., Kohler, G. O., and Garrett, W. N. (1982). "Comparative Feeding Value of Alfalfa Press Cake Residues after Mechanical Extraction of Protein." *J. Anim. Sci.*, 55(3), 498-504. DOI: 10.2134/jas1982.553498x

Woodward, W. T. W. (2008). "The Potential of Alfalfa, Switchgrass and Miscanthus As Biofuel Crops in Washington."In: *Proceedings Washington State Hay Grower Association Annual Conference and Trade Show,* Three Rivers Convention Center, Kennewick.

Xiu, S., and Shahbazi, A. (2013). "Green Biorefining of Green Biomass."In: *Biomass Processing, Conversion and Biorefinery*, B. Zhang, and Y. Wang, eds., Nova Science Publishers, Inc., Hauppauge, NY, 435-446.

Xiu, S. N., Shahbazi, A., Croonenberghs, J., and Wang, L. J. (2010). "Oil Production from Duckweed by Thermochemical Liquefaction." *Energy Sources, Part A: Recovery, Utilization, and Environmental Effects*, 32(14), 1293-1300. DOI: 10.1080/15567030903060408

Designing Broadband over Power Lines Networks Using the Techno-Economic Pedagogical (TEP) Method – Part I: Overhead High Voltage Networks and Their Capacity Characteristics

Athanasios G. Lazaropoulos [1,2,*]

1: School of Electrical and Computer Engineering, National Technical University of Athens (NTUA), 9 Iroon Polytechniou Street, Zografou, Athens, Greece 15780
2: Department of Electrical Engineering Educators, School of Pedagogical and Technological Education (ASPETE), Station Eirini HSAP, Heraklio Attikis, Athens, Greece 14121

This pair of papers proposes the techno-economic pedagogical (TEP) method that is suitable for designing Broadband over Power Lines (BPL) networks in transmission and distribution power grids. During the presentation of TEP method, a review of the recent research efforts concerning BPL networks across transmission and distribution power grids is given.

In this first paper, TEP method demonstrates to undergraduate electrical and computer engineering (ECE) students the interaction between two apparently irrelevant fields of their ECE program: Microwave Engineering and Engineering Economics. On the basis of a set of linear simplifications and suitable techno-economic metrics concerning transmission and capacity properties of overhead High Voltage Broadband over Power Lines (HV/BPL) networks, TEP method reveals the broadband potential of overhead HV/BPL networks to ECE students when different overhead HV/BPL topologies, electromagnetic interference (EMI) regulations and noise conditions are considered.

Nomenclature and Abbreviations

Nomenclature	Abbr.	Nomenclature	Abbr.
Smart Grid	SG	Differential Modes	DMs
Electrical and Computer Engineering	ECE	Wire-to-Wire	WtW
Broadband over Power Lines	BPL	Wire-to-Ground	WtG
High-Voltage	HV	Electromagnetic Compatibility	EMC
Techno-Economic Pedagogical	TEP	Injected Power Spectral Density	IPSD
Multiconductor Transmission Line	MTL	Additive White Gaussian Noise	AWGN
Electromagnetic Interference	EMI	Multiple-Input Multiple-Output	MIMO
Transmission Line	TL	Supervisory Control and Data Acquisition	SCADA
Common Mode	CM		

I. Introduction

Modern microwave engineering refers to the study and design of microwave circuits, components and systems as well as the characterization of corresponding

phenomena like noise, nonlinear effects, etc. Fundamental principles of electromagnetics, such as Maxwell's equations, wave propagation, network analysis and other design principles, are applied to analysis, design and measurement techniques in this field [1]. In fact, a plethora of microwave engineering applications emphasizes the widespread use of microwave technology for communications systems, wireless local area networks and many other systems related to the information infrastructure and the SG transition [2].

Except for the understanding of the fundamentals of microwave engineering, undergraduate ECE students should consider the economic impact and viability of each potential application along with its technical aspects. Engineering economics is the required subset of the economics that is applied to engineering projects [3]. To promote the interaction between these two fields of the ECE program –*i.e.*, Microwave Engineering and Engineering Economics–, the teaching method of case studies, which has been widely applied in relevant engineering, economic and management fields, is also applied in this paper [4]-[7].

Based on the case study of the deployment of overhead BPL networks across the overhead transmission –*i.e.*, HV– and distribution power grids, the new TEP method that is suitable for designing these overhead BPL networks is proposed. TEP method maintains its simplicity in understanding from ECE students without, however, losing its conceptual contact with the microwave engineering phenomena that characterize the propagation and transmission characteristics in overhead BPL networks. In this paper, TEP method focuses on the design of overhead HV/BPL networks [8]-[11].

TEP method combines the well-verified hybrid method, which is usually employed to examine the behavior of BPL transmission channels installed on MTL structures [8]-[17], with a set of linear simplifications, which concerns the operation of overhead HV/BPL networks. More specifically, the hybrid method, which is a careful cascade of well-known microwave engineering techniques, comprises: (i) *the bottom-up approach*: It combines MTL theory with similarity transformations determining the excited modes of overhead HV MTL configurations in terms of their propagation constants; and (ii) *the top-down approach*: It consists of the concatenation of multidimensional *T*-matrices of network modules (TM2 method) having as outputs some important techno-economic metrics of overhead HV/BPL networks such as end-to-end channel attenuation and capacity. As it is verified in this paper, the set of linear simplifications transforms the complicated hybrid method into a straightforward process without seriously affecting the validity and the accuracy of the used techno-economic metrics.

On the basis of the aforementioned two techno-economic metrics, the diverse nature of overhead HV/BPL networks is reviewed and highlighted in the 3-30MHz frequency band [10], [12]-[16]. The main contribution of TEP method is that permits to ECE students to clearly and intuitively understand the impact of several factors such as the length of overhead HV/BPL networks, the imposed power constraints in order to comply with EMI regulations concerning BPL emissions and the noise conditions. Finally, the simplicity of TEP method allows its easy implementation in computers, the further experimentation by ECE students and the familiarization of ECE students with the fundamentals of engineering economics such as the trade-off relations among involved BPL system parameters.

The rest of this paper is organized as follows: In Section II, the overhead HV configuration adopted in this paper is illustrated. Section III synopsizes the main features of overhead HV/BPL transmission. Section IV reviews the EMI regulations, the noise

characteristics and the evaluation of the capacity delivered by overhead HV/BPL networks. In Section V, numerical results and conclusions are provided, aiming at revealing the interaction of Microwave Engineering with Engineering Economics. Section VI concludes this paper.

II. A Brief Overview of Overhead HV MTL Configurations

Overhead HV MTL configurations are mainly classified in the electrical power industry by: (i) their voltage level; (ii) their number of MTL circuits per each tower; and (iii) the number of neutral conductors per each tower [8]-[11].

A typical case of 150kV single-circuit overhead HV MTL configuration is depicted in Fig. 1. Three parallel phase conductors spaced by Δ_p^{150kV} are suspended at heights h_p^{150kV} above lossy ground –conductors 1, 2 and 3–. Moreover, two parallel neutral conductors spaced by Δ_n^{150kV} hang at heights h_n^{150kV} –conductors 4 and 5– (for more details see in [8], [11]). This three-phase five-conductor ($n = 5$) overhead HV MTL configuration is considered in the present work consisting of ACSR GROSBEK conductors [10], [11], [18], [19].
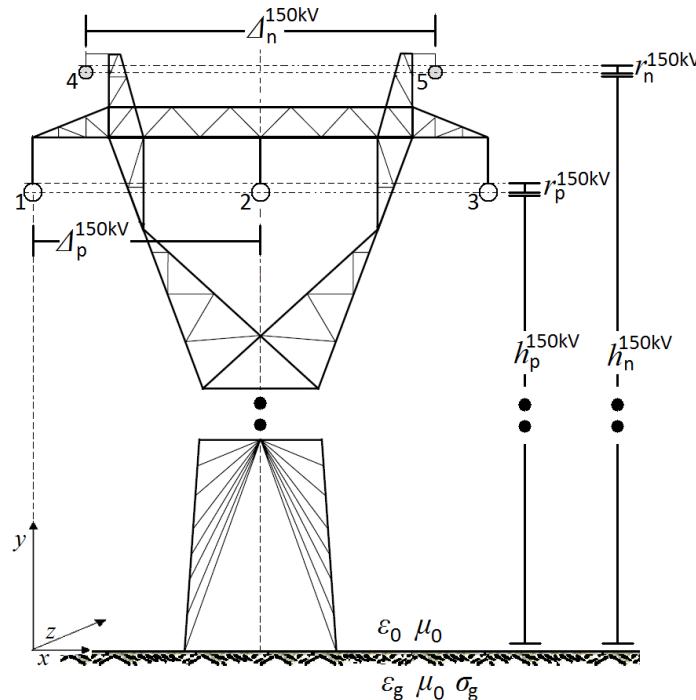
Figure 1. 150kV single-circuit overhead HV MTL structure [8], [10], [11], [18], [19].

The impact of imperfect ground on signal propagation via overhead HV/BPL networks was analyzed in [8]-[16], [20]-[23]. In accordance with these analyses, the ground is considered as the reference conductor. Its conductivity σ_g is assumed equal to

5mS/m while its relative permittivity ε_{rg} is assumed equal to 13, which is a realistic scenario [8]-[11], [13], [15], [20].

III. The Modal Analysis of Overhead HV/BPL Networks through the Prism of Hybrid and TEP Method

According to microwave engineering, the standard TL theory bridges the gap between field analysis and basic circuit theory when the phenomenon of wave propagation on TLs is examined [2]. Already analyzed in [8]-[16], through a matrix approach, the standard TL analysis can be treated as a subcase of the MTL case that involves more than two conductors. Compared to a two-conductor line supporting one forward- and one backward-traveling wave, an overhead HV MTL structure with n conductors parallel to the z axis as depicted in Fig 1 may support n pairs of forward- and backward-traveling waves with corresponding propagation constants. Each pair of forward- and backward-traveling waves is referred to as a mode.

A. Modal Propagation Constants

The n modes that are supported by the overhead HV MTL configuration of Fig. 1 are: (i) the CM where γ_{CM} constitutes its propagation constant; and (ii) the n-1 DMs (DM_{i-1} , $i=2,\ldots,n$) where γ_{DMi-1} , $i=2,\ldots,n$ constitute the propagation constants of DM_{i-1}, $i=2,\ldots,n$, respectively. The spectral behavior of the modal propagation constants has been thoroughly investigated in [8]-[11]. In Fig. 2(a), the attenuation coefficients $\alpha_{CM}=\mathrm{Re}\{\gamma_{CM}\}$ and $\alpha_{DMi-1}=\mathrm{Re}\{\gamma_{DMi-1}\}$, $i=2,\ldots,n$ of the CM and the n-1 DMs, respectively, which are evaluated using the hybrid method, are plotted versus frequency for the overhead HV MTL configuration depicted in Fig. 1. In Fig. 2(c), the phase delays $\beta_{CM}=\mathrm{Im}\{\gamma_{CM}\}$ and $\beta_{DMi-1}=\mathrm{Im}\{\gamma_{DMi-1}\}$, $i=2,\ldots,n$ of the CM and the n-1 DMs, respectively, which are evaluated using the hybrid method, are plotted versus frequency for the same configuration. Note that $\mathrm{Re}\{\cdot\}$ and $\mathrm{Im}\{\cdot\}$ returns the real and the imaginary part of a complex number, respectively.

To bypass the complicated propagation analysis of the bottom-up approach of the hybrid method and to increase the ECE students' intuitiveness of the following techno-economic analysis, TEP method proposes that the attenuation coefficients and the phase delays of the CM and the DMs can be replaced by their respective linear approximations with satisfactory accuracy. Therefore, the mean values of the attenuation coefficients of the CM and the n-1 DMs are plotted versus frequency in Fig. 2(b) while the results of applying the linear regression to the phase delays of the same modes are plotted versus frequency in Fig 2(d).

B. Modal Transfer Functions

As it has already been presented in [8]-[16], TM2 method that is subcomponent of the top-down approach of the hybrid method, which is based on the scattering matrix theory of microwave engineering and detailed in [8], models the modal spectral behavior between $V_i^{\mathrm{m}}(z)$, $i=1,\ldots,n$ and $V_j^{\mathrm{m}}(0)$, $j=1,\ldots,n$ proposing operators $H_{i,j}^{\mathrm{m}}\{\cdot\}$, $i,j=1,\ldots,n$ so that

$$\mathbf{V}^{\mathrm{m}}(z) = \mathbf{H}^{\mathrm{m}}\{\mathbf{V}^{\mathrm{m}}(0)\} \qquad (1)$$

where $\mathbf{V}^{\mathrm{m}}(z) = \begin{bmatrix} V_1^{\mathrm{m}}(z) & \cdots & V_n^{\mathrm{m}}(z) \end{bmatrix}^{\mathrm{T}}$ are the modal voltages for the given overhead HV MTL configuration corresponding to the aforementioned n supported modes, $[\cdot]^{\mathrm{T}}$ denotes the transpose of a matrix, $\mathbf{H}^{\mathrm{m}}\{\cdot\}$ is the $n \times n$ modal transfer function matrix whose elements $H_{i,j}^{\mathrm{m}}\{\cdot\}$, $i,j = 1,\ldots,n$ with $i = j$ are the modal co-channel transfer functions, while those $H_{i,j}^{\mathrm{m}}\{\cdot\}$, $i,j = 1,\ldots,n$ with $i \neq j$ are the modal cross-channel transfer functions and $H_{i,j}^{\mathrm{m}}$ denotes the element of matrix $\mathbf{H}^{\mathrm{m}}\{\cdot\}$ in row i of column j. A strong aspect of TEP method is that achieves to totally bypass the top-down approach by appropriately scaling modal propagation constants since it focuses only on overhead HV/BPL topologies without branches (see also in Section V).
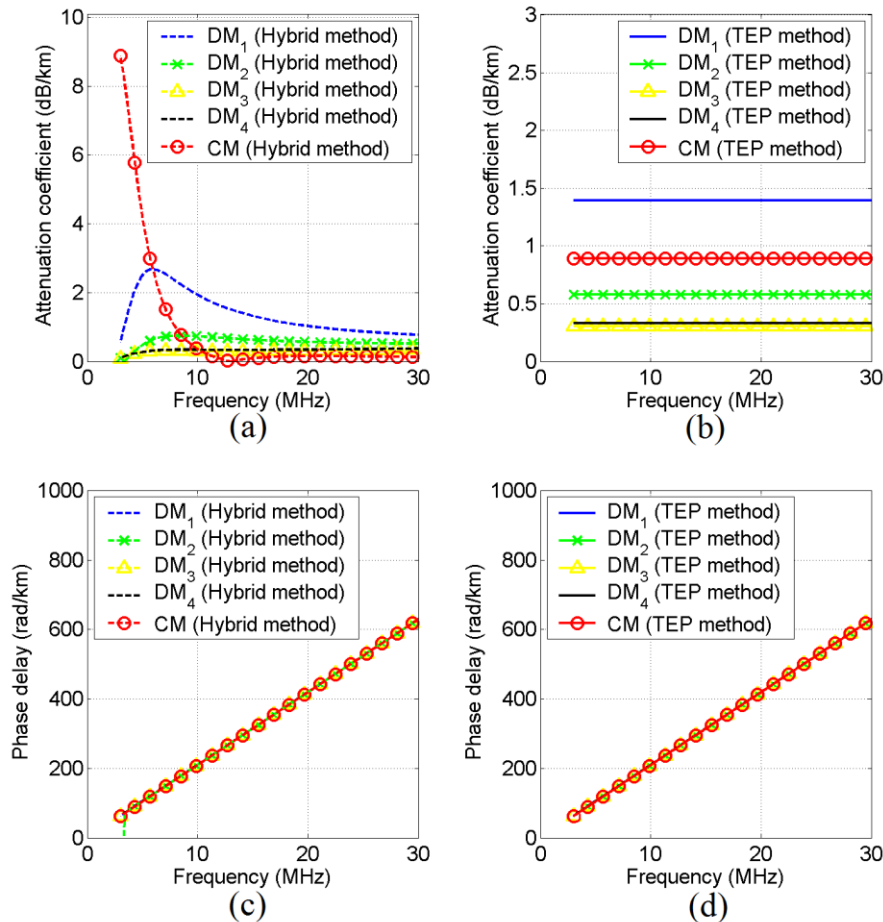
Figure 2. Frequency spectra of an 150 kV single-circuit overhead HV multiconductor structure when different methods are applied in the 3-30MHz frequency band (the subchannel frequency spacing is equal to 0.1 MHz). (a, b) Attenuation coefficients. (c, d) Phase delays.

C. Transfer Functions and Coupling Matrices

Based on the modal analysis of Section IIIB and eq. (1), the $n \times n$ transfer function matrix $\mathbf{H}\{\cdot\}$ relating $\mathbf{V}(z)$ with $\mathbf{V}(0)$ through

$$\mathbf{V}(z) = \mathbf{H}\{\mathbf{V}(0)\} \tag{2}$$

is determined from

$$\mathbf{H}\{\cdot\} = \mathbf{T_V} \cdot \mathbf{H^m}\{\cdot\} \cdot \left[\mathbf{T_V}\right]^{-1} \tag{3}$$

where $\mathbf{V}(z) = \left[V_1(z) \quad \cdots \quad V_n(z)\right]^{\mathrm{T}}$ are the line voltages for the given overhead HV MTL configuration and $\mathbf{T_V}$ is $n \times n$ matrix depending on the overhead HV MTL configuration, the frequency and the physical properties of the cables [8]-[16].

According to how signals are injected onto overhead HV/BPL TLs, two different coupling schemes exist, namely: (i) *WtW coupling schemes*, when the signal is injected between two conductors. This type of coupling scheme is outside of the scope of the TEP method; and (ii) *WtG coupling schemes*. When the signal is injected onto one conductor and returns via the ground; say between conductor s, $s=1,\ldots,n$ and the ground. Then, the coupling WtG transfer function $H^{\mathrm{WtG}}\{\cdot\}$ is given from [8]-[12]

$$H^{\mathrm{WtG}}\{\cdot\} = \mathbf{A}^{\mathrm{WtG}} \cdot \mathbf{H^m}\{\cdot\} \cdot \mathbf{B}^{\mathrm{WtG}} \tag{4}$$

where

$$\mathbf{A}^{\mathrm{WtG}} = \left[\mathbf{C}^{\mathrm{WtG}}\right]^{\mathrm{T}} \cdot \mathbf{T_V} \tag{5.1}$$

$$\mathbf{B}^{\mathrm{WtG}} = \left[\mathbf{T_V}\right]^{-1} \cdot \mathbf{C}^{\mathrm{WtG}} \tag{5.2}$$

are the coupling matrices related to the applied coupling scheme and overhead HV MTL configuration and $\mathbf{C}^{\mathrm{WtG}}$ is the $n \times 1$ WtG coupling column vector with zero elements except in the row s where the value is equal to 1 [24]. WtG coupling between conductor s and ground will be denoted as WtG^s, hereafter.

Actually, $\mathbf{A}^{\mathrm{WtG}} = \left[A_1^{\mathrm{WtG}} \quad \cdots \quad A_n^{\mathrm{WtG}}\right]$ and $\mathbf{B}^{\mathrm{WtG}} = \left[B_1^{\mathrm{WtG}} \quad \cdots \quad B_n^{\mathrm{WtG}}\right]^{\mathrm{T}}$ are $1 \times n$ coupling row vector and $n \times 1$ WtG coupling column vector, respectively, describing the contribution of each modal transfer function to the WtG coupling scheme one. The absolute value of real and the imaginary part of the elements of coupling matrix $\mathbf{A}^{\mathrm{WtG}}$ are plotted versus frequency in Figs. 3(a) and 3(b), respectively, when WtG^1 coupling scheme is applied and the hybrid method is adopted. In Figs. 3(c)-(i), the same plots are given in the case of WtG^2, WtG^3, WtG^4 and WtG^5 coupling schemes, respectively.

Similarly to the modal propagation constants, in order to completely bypass the application of the hybrid method and to simplify the following techno-economic analysis to ECE students, TEP method argues that the real parts of the elements of coupling matrix $\mathbf{A}^{\mathrm{WtG}}$ can be replaced by their mean values while their imaginary parts can be assumed equal to 0 in the frequency range of BPL operation. Hence, in Figs. 3(a)-(i), the same curves are plotted when TEP method is adopted. Same approximations are assumed in the case of the real and imaginary parts of the elements of the coupling matrix $\mathbf{B}^{\mathrm{WtG}}$.

From Figs. 2(a)-(d) and 3(a)-(j), it is evident that TEP method achieves to straightforward and efficiently describe all the propagation parameters involved in the determination of coupling WtG transfer functions of eq. (4). Actually, the propagation parameters of TEP method can be available *ab initio* for given overhead HV MTL

configuration and WtG coupling scheme. However, the overall performance of TEP method needs to be verified against other well-validated results, such as those derived from the hybrid method, for different techno-economic metrics (see in Section V).

IV. The Capacity Analysis of Overhead HV/BPL Networks Using the Hybrid and TEP Method

Based on suitable techno-economic metrics, such as end-to-end channel attenuation and capacity of this paper, ECE students can assess the performance of overhead HV/BPL networks through the TEP method and, at the same time, TEP method can facilitate the design of overhead HV/BPL networks. More specifically, as it concerns the end-to-end channel attenuation, the propagation analysis of Section III is sufficient.
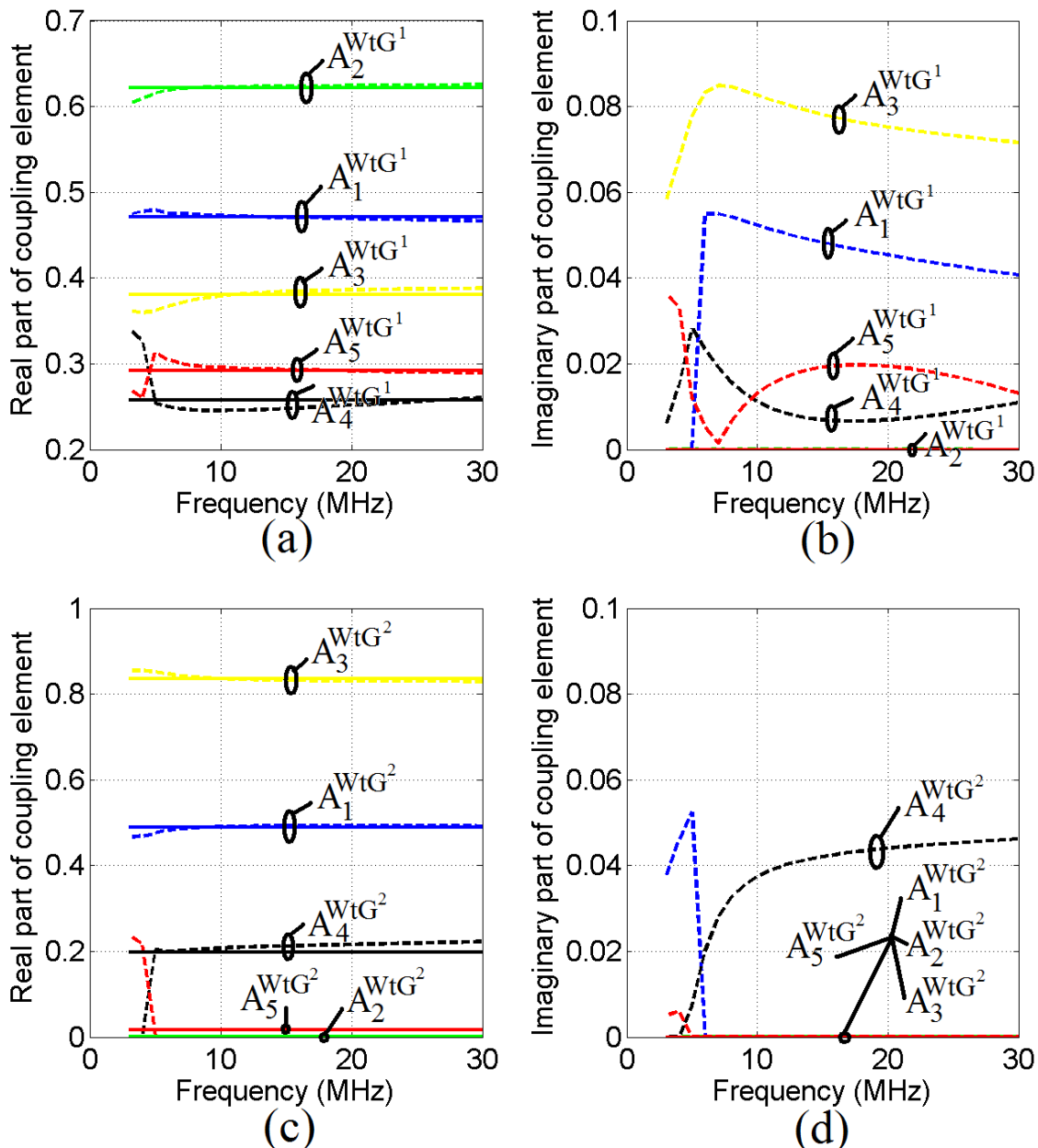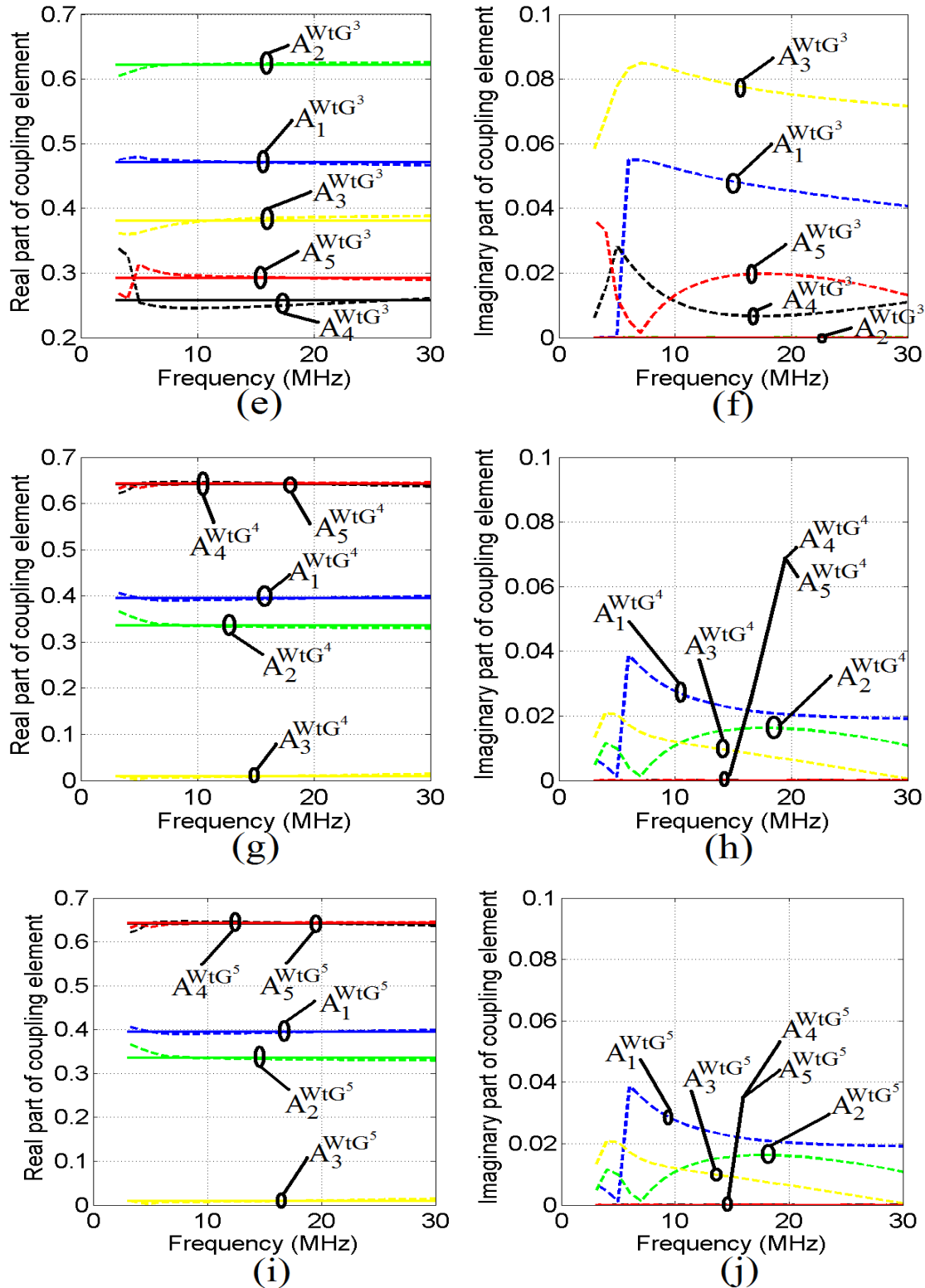
Figure 3. Spectral behavior of coupling elements of A^{WtG} for different WtG coupling schemes when the hybrid method (dashed lines) and the TEP method (solid lines) are applied in the 3-30MHz frequency band (the subchannel frequency spacing is equal to 0.1 MHz). (a,c,e,g) Absolute value of real parts. (b,d,f,h) Absolute value of imaginary parts.

Nonetheless, except for this propagation analysis, a set of properties regarding the spectral efficiency of overhead HV/BPL networks, such as EMI regulations and noise, is required so that the capacity of these networks can be evaluated. In fact, TEP method exploits the already simplified and well-verified spectral efficiency properties of the hybrid method.

A. EMC with other Radio services. EMI Regulations and Respective Power Constraints

Since overhead HV/BPL networks may become both a source and a victim of EMI, a critical issue related to BPL technology has to do with the power constraints that should be imposed to ensure successful BPL coexistence with other already existing wireless and telecommunications systems [12], [15], [16], [25], [26]. Among regulatory bodies that have established regulations concerning BPL network operation and the corresponding emissions from BPL equipment, the most important are: (i) *Regulations from national bodies*: FCC Part 15, German Reg TP NB30, the Norwegian Proposal and the BBC/NATO Proposal [27]-[31]; and (ii) *Regulations from BPL equipment manufacturers*: IEEE proposal and HomePlug AV proposal [32], [33].

The comprehensive compliance testing procedures require electromagnetic field measurements at each BPL unit being part of the BPL network. As it has already presented in [9], [12], [15], [16], a simpler regulatory approach would be to avoid formal compliance tests by limiting IPSD to a level that, in most circumstances, does not produce EMI exceeding certain limits. Among the different IPSD limits proposals, the IPSD limits proposed by Ofcom for compliance with FCC Part 15 –presented in [27]-[31]– are the most cited. More specifically, for overhead HV/BPL networks, according to Ofcom, in the 3-30MHz frequency range maximum levels of -60 dBm/Hz constitute appropriate IPSD limits $p(f)$ providing presumption of compliance with the current FCC Part 15 limits [9], [12], [15], [16], [31], [34], [35].

As it concerns the EMI regulations from national bodies, the electromagnetic field strength limits proposed by FCC Part 15, German Reg TP NB30, the Norwegian Proposal and the BBC/NATO Proposal are presented in [27], [29], [30]. Since Ofcom/FCC Part 15 IPSD limits are well defined, the respective IPSD limits of German Reg TP NB30, the Norwegian Proposal and the BBC/NATO Proposal can easily be determined [30].

As it concerns the IPSD limits from BPL equipment manufacturers, those of IEEE and HomePlug AV are well known and are presented in [32], [33]. However, these IPSD limits are not always EMI-harmless to other already existing telecommunications systems.

B. Noise Characteristics

According to [12], [15], [16], [20], [24], [36]-[38], two types of noise are dominant in overhead HV/BPL networks: (i) *Colored background noise.* It is the environmental noise depending on weather conditions, humidity, geographical location, height of cables above the ground, corona discharge, e.t.c.; and (ii) *Narrowband noise.* It is the result of narrowband interference from other wireless services operating at the same frequency range with overhead HV/BPL networks.

In accordance with [9], [12], as it regards the noise properties of overhead HV/BPL networks in the 3-30MHz frequency band, uniform AWGN PSD level $N(f)$ is assumed. Thoroughly examining the existing BPL noise literature [12], [15], [16], [20], [24], [34], [35], [38], these uniform AWGN/PSD levels may vary from –95dBm/Hz (bad

noise scenario) to –115dBm/Hz (good noise scenario) with average value equal to –105dBm/Hz (average noise scenario). In very special cases of severe weather and aggravated EMI conditions, it is reported that AWGN/PSD levels can reach up to –50dBm/Hz (very bad noise scenario).

Note that as it regards the above noise characteristics of overhead HV/BPL networks, common AWGN PSD level $N(f)$ is assumed for the different modal and coupling scheme channels exploiting their significant similarities concerning BPL signal transmission. Anyway, this is a typical procedure that does not harm the generality of the following analysis [15], [20], [24], [39].

C. Capacity

Capacity is the maximum achievable transmission rate over a BPL channel –either modal or coupling scheme one–. It depends on the overhead HV MTL configuration, overhead HV/BPL topology, the applied coupling scheme, the imposed EMI regulations and the noise characteristics. More specifically, the capacity of an overhead HV/BPL channel is given by [9], [12], [15], [16], [40]-[42]

$$C \equiv C(L = K) = f_s \sum_{q=0}^{L-1} \log_2 \left\{ 1 + \left[SNR(3\text{MHz} + qf_s) \cdot |H(3\text{MHz} + qf_s)|^2 \right] \right\} \quad (6)$$

$$SNR(f) = \langle p(f) \rangle_L / \langle N(f) \rangle_L \quad (7)$$

$$K = (30 - 3)\text{MHz} / f_s \quad (8)$$

where $H\{\cdot\}$ is the transfer function of either modal or coupling scheme channel considered, $\langle \cdot \rangle_L$ is an operator that converts dBm/Hz into a linear power ratio (W/Hz), K is the number of subchannels in the BPL signal frequency range of interest and f_s is the flat-fading subchannel frequency spacing.

The cumulative capacity is defined as the cumulative upper limit of information which can reliably be transmitted over the overhead HV/BPL channel. For given frequency $f \in [3, 30]$ MHz, overhead HVMTL configuration and coupling scheme configuration and taking into account eq. (6), cumulative capacity is determined by [40]-[42]

$$CumC(f) = C\left(L = \left\| \frac{f - 3\text{MHz}}{f_s} \right\| + 1 \right) \quad (9)$$

where $\|x\|$ is the nearest integer to x. In fact, cumulative capacity describes the aggregate capacity effect of all subchannels of the examined frequency band.

V. Numerical Results and Discussion

The simulation results of various types of overhead HV/BPL channels aim at highlighting to ECE students: (i) their broadband performance; (ii) how their capacity is influenced by various inherent and imposed factors; (iii) the influence of EMI regulations and noise conditions on the used techno-economic metrics; and (iv) the adaptive capacity mitigation technique that redefines the EMI regulations by taking into account noise conditions. Prior to study the previous findings, the significant convergence between hybrid and TEP method needs to be examined.

As mentioned in Section III, since the modes supported by the overhead HV MTL configurations may be examined separately, it is assumed for simplicity that the BPL signal is injected directly into the existing EVD modes [8]-[17], [20], [34], [43]; thus, either the complicated modal analysis of [34], briefly described in Section III, is bypassed or the proposed approximations of TEP method can comfortably be applied.

For the numerical computations, the 150kV single-circuit overhead HV MTL configuration, depicted in Fig. 1, has been considered. In order to apply the hybrid and TEP method, according to the hybrid method, a general end-to-end BPL connection is separated into segments –network modules–, each of them comprising the successive branches encountered –see Figs. 4(a) and 4(b)–. However, the TEP method copes with overhead HV/BPL networks that comprise "LOS" transmission topologies where "LOS" topologies correspond to Line-of-Sight transmission of wireless channels (*i.e.*, no branches are encountered). Hence, the "LOS" transmission along the average end-to-end distance $L=L_1+\ldots+L_{N+1}=25$km is assumed. Finally, with reference to Fig. 4(b), the transmitting and the receiving ends are assumed matched to the characteristic impedance of the supported modal channels [9]-[16], [18], [20], [45].

A. Modal and Coupling Scheme Channels of Hybrid and TEP Method: Their Converged Transmission and Capacity Performance

The following discussion will focus on the transmission and capacity characteristics using the techno-economic metrics of end-to-end channel attenuation and cumulative capacity associated with: (i) the CM and the DMs of the aforementioned overhead HV MTL configuration; and (ii) the WtG coupling schemes related to this overhead HV MTL configuration.

As it has already been presented in [9]-[11], to verify the convergence between hybrid and TEP method and to compare modal channels with coupling scheme ones, a representative overhead HV/BPL topology of path length up to 25km is examined, namely:

(1) The "LOS" transmission along the average end-to-end distance $L=L_1+\ldots+L_{N+1}=25$km when no branches are encountered (case A).

With respect to Fig. 4(a) and as it concerns the transmission characteristics of overhead HV/BPL channels, in Fig. 5(a), the end-to-end channel attenuation from A to B is plotted versus frequency in the 3-30MHz frequency band for the propagation of CM and DM_{i-1}, $i=2,\ldots,5$ when the 150kV single-circuit overhead HV MTL configuration is considered and hybrid method is applied. In Fig. 5(b), the same plots are given when the TEP method is adopted.

In Fig. 5(c), the end-to-end channel attenuation from A to B for the "LOS" transmission case A is plotted versus frequency when the hybrid method is adopted for the following coupling schemes: WtG^1, WtG^2, WtG^3, WtG^4 and WtG^5. In Fig. 5(d), the same curves are plotted when the TEP method is applied.
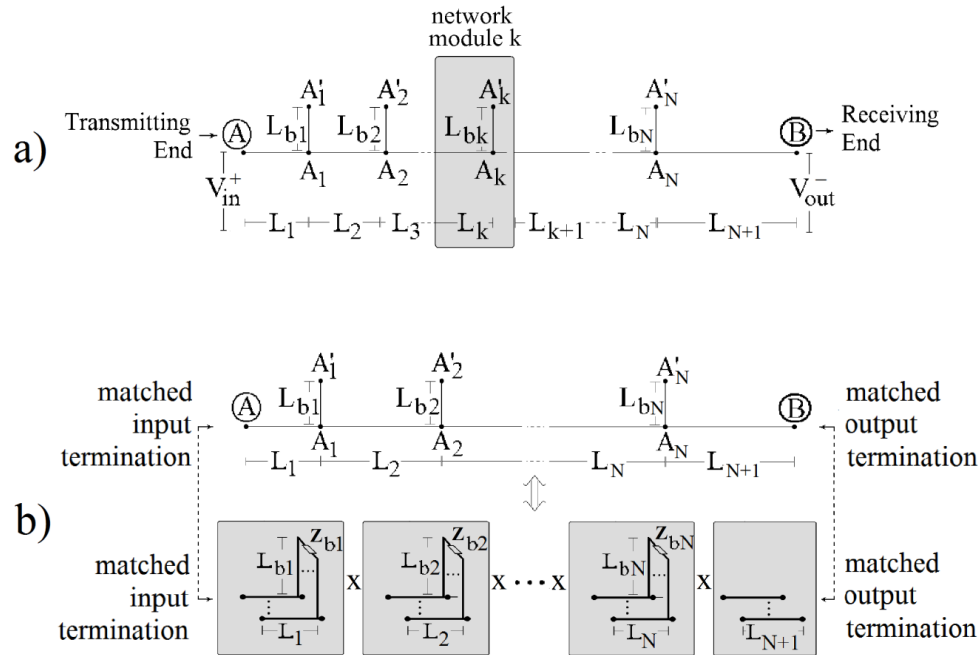
Figure 4. End-to-end BPL connection with *N* branches. (b) In accordance with the hybrid method, an indicative overhead HV/BPL topology considered as a cascade of *N*+1 modules corresponding to *N* branches [8]-[16].

At the same time, to investigate the capacity potential of overhead HV/BPL channels, in Fig. 6(a), the cumulative capacity of the aforementioned five modes is plotted with respect to frequency in the 3-30MHz frequency band when the 150kV single-circuit overhead HV MTL configuration, FCC Part 15 limits and average noise scenario are considered and the hybrid method is adopted. In Fig. 6(b), the same plots are given when the TEP method is applied.

In Figs. 6(c) and 6(d), similar plots are given in the case of the aforementioned indicative coupling schemes when the hybrid and TEP method is adopted, respectively.

From Figs. 5(a)-(d) and 6(a)-(d), several interesting remarks regarding transmission and capacity properties of overhead HV/BPL networks can be highlighted to ECE students:

- The simulation results of the average length "LOS" transmission channels reveal the potentially excellent communications medium of overhead HV/BPL channels –either modal or coupling scheme ones–. Already verified in [10], [12], [15], [16], [18], the entire overhead transmission power grid resembles a flat-fading transmission system with low-loss and high-capacity characteristics revealing an attractive broadband last mile alternative and SG telecommunications solution.
- As it concerns the end-to-end attenuation of modal and coupling scheme channels, TEP method achieves to provide a satisfactory approximation of their actual behavior, as verified by the hybrid method. The great success of the TEP method is that it holds this attenuation accuracy in comparison with the hybrid method results bypassing the complicated bottom-up and top-down approaches of the
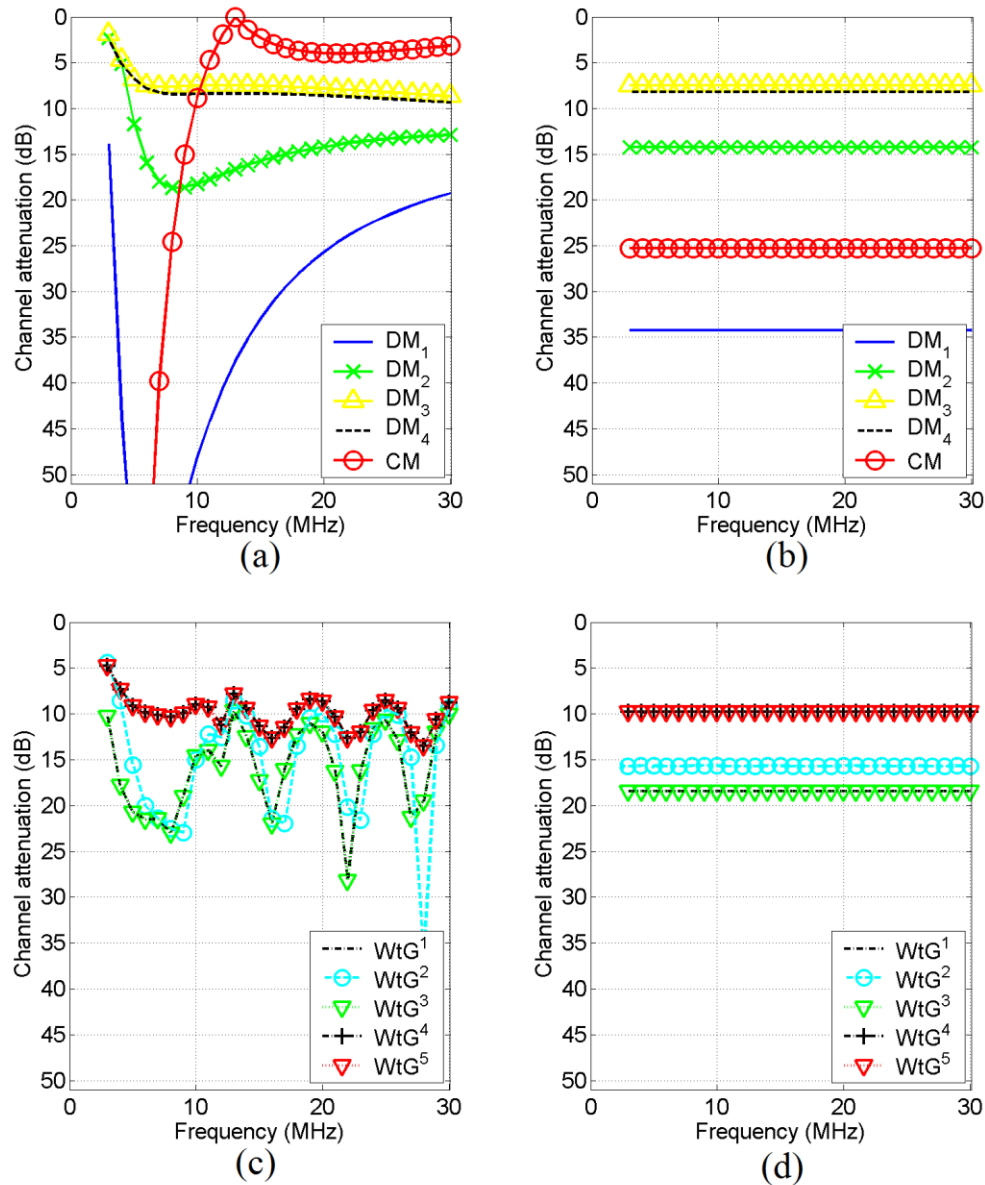
Figure 5. Channel attenuation versus frequency for the "LOS" transmission case A when the 150kV single-circuit overhead HV MTL configuration, FCC Part 15 limits and average noise scenario are assumed (for plot clarity reasons, the subchannel frequency spacing is equal to 1MHz). (a) End-to-end attenuation of modal channels (hybrid method). (b) End-to-end attenuation of modal channels (TEP method). (c) End-to-end attenuation of WtG coupling scheme channels (hybrid method). (c) End-to-end attenuation of WtG coupling scheme channels (TEP method).

hybrid method. This is achieved by simply scaling the modal propagation constant results of Figs. 2(a)-(d) and using the constant coupling elements of Figs. 3(a)-(j). For example, the results concerning the absolute value of the modal channel attenuation presented in Fig. 5(b) come from the simple multiplication of the modal attenuation constants with 25. Then, the results concerning the absolute
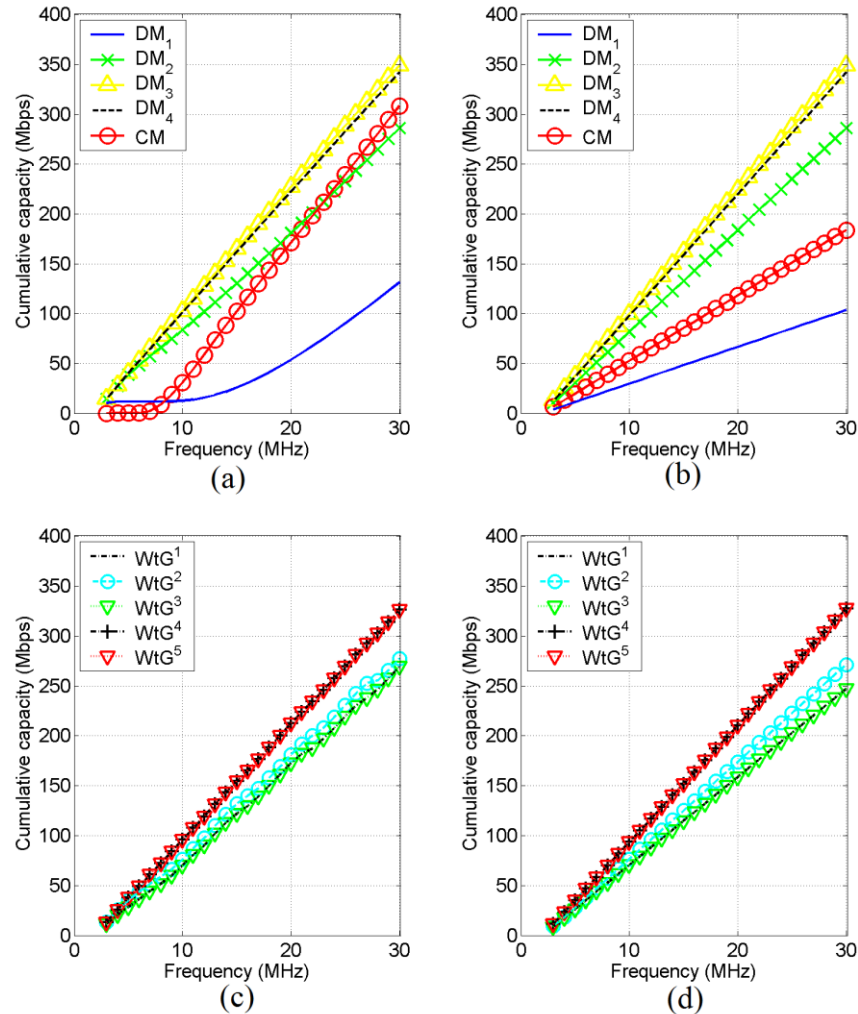
Figure 6. Cumulative capacity versus frequency for the "LOS" transmission case A when the 150kV single-circuit overhead HV MTL configuration, FCC Part 15 limits and average noise scenario are considered (for plot clarity reasons, the subchannel frequency spacing is equal to 1MHz). (a) Cumulative capacity of modal channels (hybrid method). (b) Cumulative capacity of modal channels (TEP method). (c) Cumulative capacity of WtG coupling scheme channels (hybrid method). (d) Cumulative capacity of WtG coupling scheme channels (TEP method).

value of the channel attenuations presented in Fig. 5(d) come from the straightforward multiplication of the modal channel attenuations of Fig. 5(b) with the respective coupling elements of the applied coupling scheme. Already mentioned, note that modal propagation constants and coupling elements of TEP method are already known for given overhead HV MTL configuration and coupling scheme.

- The ECE students can observe that the spectral behavior of the end-to-end modal channel attenuation critically depends on the mode and the length of the topology examined. Already identified for the hybrid method in [10], [11], [13], [15], [18], [20], the shape and depth of the end-to-end channel attenuation of CM is primarily influenced by the penetration depth into the lossy ground and the resonance occurring inside the ground, whereas the shape and depth of the

end-to-end channel attenuation of DMs is mainly affected by the losses and the skin-effect in the conductors.

- As it concerns the capacity of modal and coupling scheme channels, TEP method achieves to provide a very good approximation of their actual behaviour, as it is evaluated by the hybrid method. The main divergence between the capacity results of the hybrid and the TEP method is the CM modal capacity that is, anyway, vanished during the capacity evaluation of coupling scheme channels. Apart from the easy capacity computations due to the transmission and capacity assumptions of TEP method, ECE students can also observe the linear slope of cumulative capacity results that is explained by the constant terms included in eq. (6).

- Already mentioned in [9]-[11], as it concerns the transmission characteristics of overhead HV/BPL networks, WtG coupling schemes are mostly influenced by the CM behaviour. Here, it is validated that the same influence behaviour regarding coupling schemes and their compound modes is also observed in the case of capacity metrics. Since CM demonstrates competitive transmission and capacity results among the other supported DMs' ones, WtG coupling schemes also attain favourable results in terms of channel attenuation and cumulative capacity in comparison with other coupling schemes such as WtW ones [9], [11]. Therefore, during practical implementations in overhead HV/BPL networks, WtG coupling schemes are preferred regardless of the power grid type considered when the primary design objective is the capacity/throughput maximization.

- One of the main issues concerning the design of networks is the trade-off relations among involved system performance metrics. ECE students should understand that there are significant trade-off relations even in the design of overhead HV/BPL networks; although WtG coupling schemes present favourable channel attenuation and capacity characteristics, the significant EMI of WtG coupling schemes to other already licensed wireless communications due to CM is the main significant drawback of WtG coupling scheme system deployment [9], [11], [29], [30]. At this point, ECE students should recognize that today's EMI regulations provide the required protection between BPL systems and other radio services regardless of the coupling scheme applied.

Without affecting the generality of the analysis, only TEP method is adopted and only one of the WtG coupling schemes –say WtG^4 one– will be examined, hereafter.

B. Influence of Overhead HV/BPL Topologies on Transmission and Capacity Metrics

The potential transmission and capacity performance of overhead HV/BPL networks in terms of end-to-end channel attenuation and cumulative capacity, respectively, is evaluated based on the application of FCC Part 15 limits and the consideration of average noise scenario in the 3-30MHz frequency band when different lengths of overhead HV/BPL topologies occur.

More specifically, with reference to Fig. 4(b), similarly to the "LOS" transmission case A already presented in Section VA, other three indicative overhead HV/BPL topologies of "LOS" transmission are examined, namely:

(2) The "LOS" transmission along the average end-to-end distance $L=L_1+\ldots+L_{N+1}=1$km (case B).

(3) The "LOS" transmission along the average end-to-end distance $L=L_1+\ldots+L_{N+1}=10$km (case C).

(4) The "LOS" transmission along the average end-to-end distance $L=L_1+\ldots+L_{N+1}=100$km (case D).

As it concerns the transmission characteristics of the 150kV single-circuit overhead HV/BPL coupling scheme channels, in Fig. 7(a), the end-to-end channel attenuation from A to B is plotted versus frequency in the 3-30MHz frequency band for "LOS" transmission case A, B, C and D when WtG^4 coupling scheme is applied. In Fig. 7(b), respective curves in terms of cumulative capacity are plotted as a function of frequency in the same frequency band for the same indicative BPL topologies when WtG^4 coupling scheme is applied.

Observing Figs. 7(a) and 7(b), it is clearly demonstrated to ECE students that:

- Already verified in [9], the low-loss flat-fading transmission system with high-capacity characteristics still exist regardless of the overhead HV/BPL topology examined. Although end-to-end overhead HV connections of lengths up to 100km are examined, the corresponding capacity is equal to 109Mbps in the 3-30MHz frequency band when FCC Part 15 limits and average noise scenario are considered. In addition, these high capacity values reveal the strong broadband potential of the entire overhead HV/BPL grid.

- ECE students should understand the critical role of end-to-end distance during the design of overhead HV/BPL networks. It can be easily pointed out that "LOS" transmission case B and D define the upper and lower channel attenuation/capacity bound, respectively, in the overhead HV MTL configuration examined. Hence, only these two overhead HV/BPL topologies will be examined, hereafter, determining the capacity limits of today's overhead HV/BPL networks when different operation scenarios are examined.

C. Effect of EMI Regulations on the Capacity Performance of Overhead HV/BPL Network

In this subsection, the capacity performance of overhead HV/BPL networks is investigated taking under consideration their EMI to other licensed wireless services [12], [15], [16]. Among the proposals related to the control of EMI caused by BPL operation, the six EMI regulations of Section IVA, which are characterized by their respective IPSD limits, are examined in this subsection, namely:

(i)   the *FCC limits* proposed by FCC Part 15.
(ii)   the *German limits* proposed by German Reg. TP NB30.
(iii) the *Norwegian limits* proposed by Norway.
(iv)   the *BBC/NATO limits* proposed by BBC and NATO.
(v)   the *IEEE limits* proposed by IEEE.
(vi)   the *HomePlug limits* proposed by HomePlug AV.

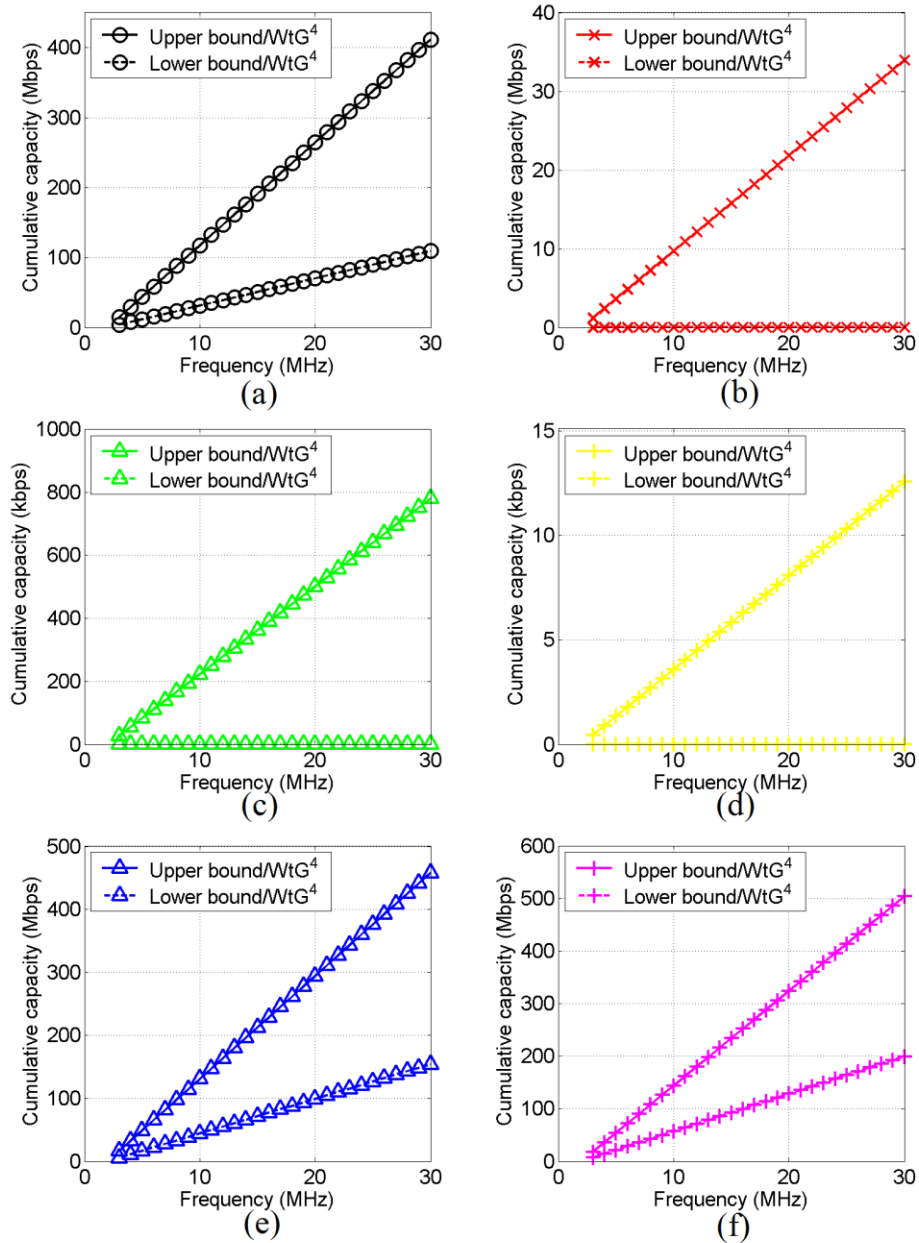In Fig. 8(a), the lower and upper cumulative capacity bounds of the 150kV single-circuit overhead HV/BPL channels have been plotted in the 3-30MHz frequency band in order to examine the effect of the FCC limits when WtG^4 coupling scheme is applied and average noise scenario is assumed. In Figs. 8(b)-(f), similar curves are given in the case of German, Norwegian, BBC/NATO, IEEE and HomePlug limits, respectively.
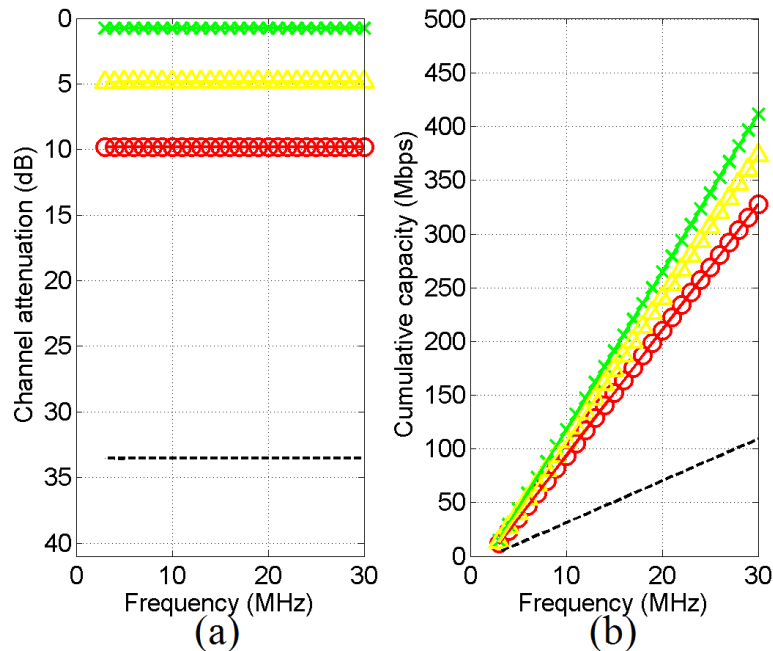
Figure 7. Transmission and capacity metrics of the 150kV single-circuit overhead HV MTL configuration versus frequency for "LOS" transmission case A (⊖), case B (✳), case C (△) and case D (▬▬) when FCC Part 15 limits and average noise scenario are considered and WtG[4] coupling scheme is applied (for plot clarity reasons, the subchannel frequency spacing is equal to 1MHz). (a) End-to-end channel attenuation. (b) Cumulative capacity.

From Figs. 8(a)-(f), several important capacity issues can be highlighted:

- ECE students can identify that the choice of EMI regulations remains a crucial decision regarding future's overhead HV/BPL broadband expansion. The tighter versions of EMI regulations combined with the very long connections push overhead HV/BPL networks to their broadband extinction; under these EMI regulations, overhead HV/BPL networks do not exhibit any capacity advantage in comparison with the vintage SCADA networks.

- In addition, ECE students can identify capacity differences of the order of hundreds of Mbps among different EMI regulations. This fact reveals the need of a slight relaxation for such long-range systems so that corresponding relaxed IPSD limits will lead to a considerable capacity increase. This adjustment may be accompanied with the use of appropriate adaptive mitigation techniques such as the adoption of different EMI regulations depending on telecommunications EMC needs, the imposition of power masking adaptive to local traffic, multi-hop transmission and cooperative communications [12], [15], [16].

- ECE students should also recognize the importance of cooperative communications. The promotion of standardized topologies concept among HV/BPL, MV/BPL and LV/BPL networks may help towards a centralized cooperative BPL network structure. This is a good reason for unveiling the need for intraoperability/interoperability of overhead HV/BPL networks with other SG broadband technologies (see also Section VE).

Figure 8. Upper and lower cumulative capacity bounds of the 150kV single-circuit overhead HV MTL configuration versus frequency when WtG^4 coupling scheme is applied for different EMI regulations (for plot clarity reasons, the subchannel frequency spacing is equal to 1MHz). (a) FCC limits. (b) German limits. (c) Norwegian limits. (d) BBC/NATO limits. (e) IEEE limits. (f) HomePlug limits.

- When relaxed EMI regulations are adopted –such as FCC, IEEE and HomePlug limits–, the occurred lower capacity bounds unveil the dynamic broadband SG character of overhead HV/BPL networks. The fact that an extended portfolio of SG applications needs no more than 15-20Mbps combined with the findings of lower capacity bounds render overhead HV/BPL lines as a very efficient SG telecommunications platform.

D. The Combined Effect of EMI Regulations and Noise Conditions on Capacity Performance of Overhead HV/BPL Networks

Apart from the EMI regulations and the *de-facto* long-range nature of overhead HV/BPL topologies, in order to design high-bitrate overhead HV/BPL networks with capacities in the range of Gbps, the detailed knowledge of the noise environments is imperative [8]-[11].

Opposite to many other broadband telecommunications systems, such as optical fiber networks, and as it has already been reported in Section IVB, overhead HV/BPL noise presents high variability. This is due to the fact that overhead HV/BPL noise depends either on inherent environmental factors or on imposed narrowband interference conditions [9], [15], [16], [20], [28], [46], [47]. Actually, the significant differences in dBm among different noise levels are reflected on respective differences in the capacity of overhead HV/BPL networks.

In fact, the combined effect of different EMI regulations with peculiar noise conditions creates important capacity fluctuations during the operation of overhead HV/BPL networks. Depending on the capacity thresholds that are imposed by various SG applications and EMI requirements, a more general EMI regulation framework may be introduced; the IPSD limits can be adaptively tuned in local or temporal basis in order to mitigate capacity losses caused by either inherent or imposed factors across overhead HV/BPL networks bypassing universal fixed strict EMI regulations.

The following discussion focuses on the spectral efficient capabilities in terms of capacity in the 3-30MHz frequency band through the application of the six EMI regulations of Section IVA when different noise environments that range from the very bad noise scenario to the good one occur. Based on the "LOS" overhead HV/BPL topologies of 1km (case B) and 100km (case D) that define the upper and lower capacity bounds, respectively, the following analysis tries to investigate: (i) the influence of different noise conditions to overall capacity; (ii) the combined impact of noise and EMI regulations on the broadband capacity performance of overhead HV/BPL networks; and (iii) the mitigation of capacity losses due to noise variability through the adoption of more relaxed EMI regulations.

In Fig. 9(a), the lower and upper capacity bounds of the 150kV single-circuit overhead HV/BPL channels in the 3-30MHz frequency band have been plotted versus uniform AWGN/PSD levels when WtG[4] coupling scheme and FCC limits are considered. The uniform AWGN/PSD levels range from –50dBm/Hz (very bad noise scenario) to –115dBm/Hz (good noise scenario). In Figs. 9(b)-(f), similar curves are given in the case of German, Norwegian, BBC/NATO, IEEE and HomePlug limits, respectively.

Observing Figs. 9(a)-(f), ECE students can deduce certain interesting conclusions:

- It is revealed how significant for BPL transmission is the noise variance and EMI regulations as well as their interaction. In fact, capacity differences of the order of hundreds of Mbps in the 3-30MHz frequency band are observed among different combinations of AWGN/PSD and IPSD levels; say, in the case of FCC limits, capacity differences up to approximately 500Mbps are observed between the best and the worst BPL transmission cases.
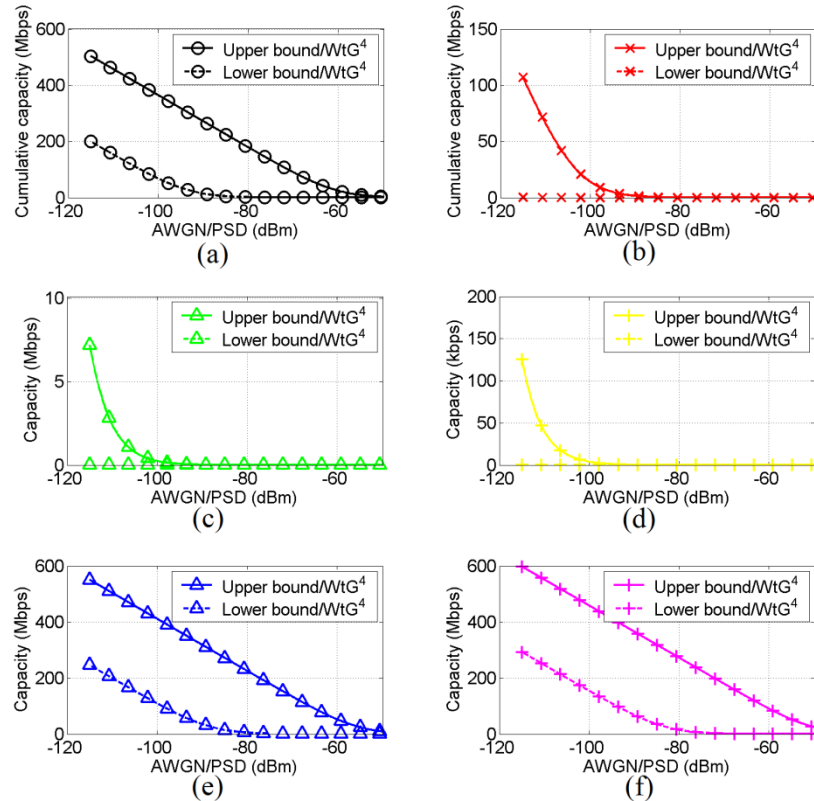
Figure 9. Upper and lower capacity bounds of the 150kV single-circuit overhead HV MTL configuration versus uniform AWGN/PSD when WtG^4 coupling scheme is applied for different EMI limits (the subchannel frequency spacing is equal to 1MHz). (a) FCC limits. (b) German limits. (c) Norwegian limits. (d) BBC/NATO limits. (e) IEEE limits. (f) HomePlug limits.

- Compared to other relevant capacity results of overhead and underground LV/BPL and MV/BPL networks [12], [15], [16], if good and average noise conditions are combined with appropriate EMI regulations, overhead HV/BPL networks present notable capacity performance permitting their operation as backbone networks. Actually, during these optimum operation conditions, overhead HV/BPL networks can concentrate local traffic from other already existing surrounding broadband networks if appropriate topologies are employed. However, before overhead HV/BPL systems interoperate with other broadband technologies –wireline, such as fiber and DSL, and wireless, such as WiFi and WiMax–, the overhead HV/BPL networks need to intraoperate with other surrounding overhead and underground MV/BPL and LV/BPL networks exploiting the scalable capacity principles [8]-[16].

- If 100km-long "LOS" transmission topologies are adopted, capacity performance of overhead HV/BPL networks is seriously damaged even if power injection is defined by the highest today's IPSD limits that respect EMC regulations –*i.e.*, FCC limits–. Numerically, when very bad noise scenario occurs and FCC limits are applied, the maximum capacity of overhead HV/BPL networks does not exceed 3.3Mbps. Therefore, the harsh noise environments that derive from either environmental factors or narrowband interference conditions pulverize overhead

HV/BPL network broadband perspective [9], [15], [16], [20], [28], [46]-[48]. Similarly to the numerical results of Section VC when severe noise conditions occur, overhead HV/BPL networks do not exhibit any capacity advantage in comparison with the SCADA networks.

E. Converting Disadvantage into Advantage: The Mitigation of Capacity Losses due to Noise Conditions Using Adaptive EMI Regulations

In Section VD, it has been clearly shown that if severe noise conditions concur with strict EMI regulations, this combination annihilates broadband capacity potential of overhead HV/BPL networks. The ECE students should understand that, reversing the arrow of IPSD limits through the appropriate adjustment of EMI regulations via their respective IPSD limits, the capacity effect of severe noise conditions can be mitigated ensuring scalable capacities among already installed overhead HV/BPL networks that are characterized by different noise conditions.

In this subsection, the adaptive adjustment of IPSD limits that depends on the weather and various EMC conditions is proposed. This capacity mitigation technique primarily ensures scalable capacities among overhead HV/BPL networks and secondarily guarantees the required symbiosis of overhead HV/BPL networks with other SG telecommunications systems. Given a capacity threshold, appropriate IPSD limits are determined so as to counterbalance capacity losses due to different AWGN/PSDs when different overhead HV/BPL topologies occur. More specifically, in order to ensure that upper and lower capacity bounds are perfectly adjusted to the required capacity threshold, appropriate upper and lower IPSD limits are determined, respectively.

In Fig. 10(a), these upper and lower IPSD limits of the 150kV single-circuit overhead HV MTL configuration in the 3-30MHz frequency band have been plotted versus uniform AWGN/PSD levels when WtG^4 coupling scheme is applied and the capacity threshold is assumed equal to 100Mbps. The uniform AWGN/PSD levels range from –95dBm/Hz (bad noise scenario) to –115dBm/Hz (good noise scenario). In Figs. 10(b)-(d), similar curves are given when the capacity threshold is assumed equal to 200Mbps, 300Mbps and 400Mbps, respectively.

Observing Figs. 10(a)-(d), the following remarks can be highlighted to ECE students:

- The schematically linear behavior of IPSD limits in respect with AWGN/PSD levels for given capacity threshold, which is observed in the previous figures, is mathematically justified by studying eqs (6) and (7); in order to maintain a fixed capacity threshold, as it is described in eq. (6), a fixed ratio between IPSD limits and AWGN/PSD levels is required. This fixed ratio, which is given in eq. (7), further entails a linear dependence relation in dB between IPSD limits and
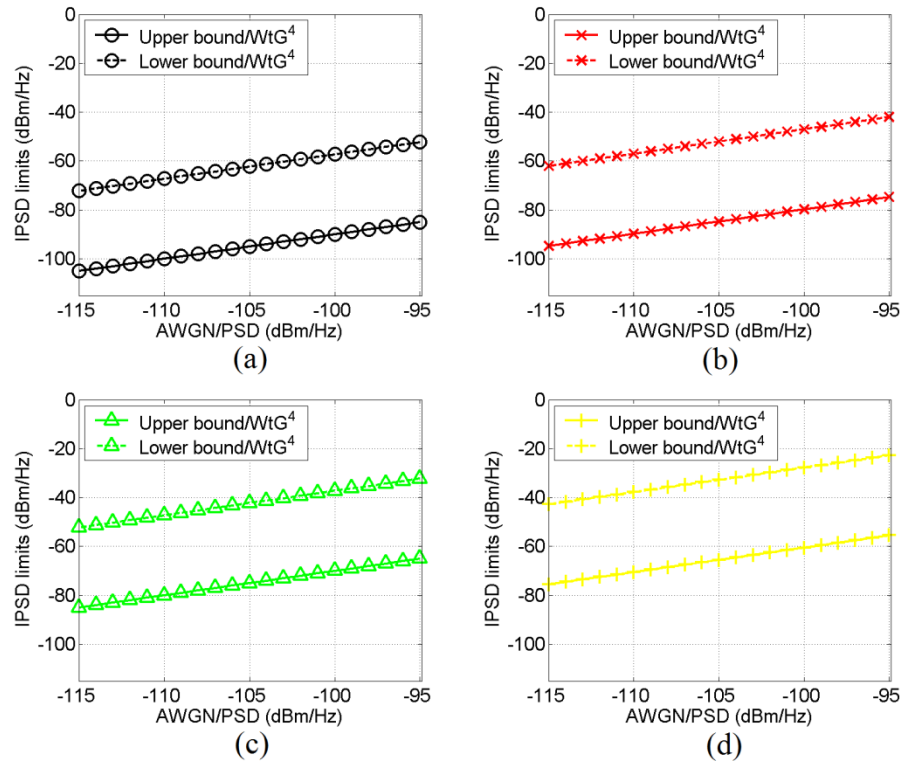
Figure 10. Upper and lower IPSD limits of the 150kV single-circuit overhead HV MTL configuration versus uniform AWGN/PSD when WtG^4 coupling scheme is applied for different capacity thresholds (the subchannel frequency spacing is equal to 1MHz). (a) Capacity threshold of 100Mbps. (b) Capacity threshold of 200Mbps. (c) Capacity threshold of 300Mbps. (d) Capacity threshold of 400Mbps.

AWGN/PSD levels. Therefore, capacity losses or gains due to weather and EMI conditions can be efficiently regulated by appropriately raising or decreasing IPSD limits, respectively. The level of IPSD limits adjustment can be accurately estimated using either the mathematical analysis based on Section IVC or schematic rules of thumb such as those of Figs. 10(a)-(d).

- It is obvious that the lower capacity bounds of overhead HV MTL configurations require higher IPSD limits in comparison with the upper capacity bounds so that a common capacity threshold among different overhead HV/BPL topologies can be ensured. Moreover, as the capacity threshold raises and/or noise conditions deteriorate, so do the respective upper and lower IPSD limits.

- By appropriately adjusting IPSD limits, a great number of capacity thresholds can be set regardless of the considered overhead HV MTL configuration and the noise environment. Hence, the concept of scalable capacity among overhead HV/BPL networks is comfortably ensured through this adaptive capacity mitigation technique. Anyway, this capacity countermeasure, which defines a strong techno-economic design tool, permits the further coexistence among overhead HV/BPL networks of different overhead HV/BPL topologies.

- Despite the fact that every capacity threshold can theoretically be achieved across a transmission BPL network by simply tuning IPSD limits across its compound overhead HV/BPL networks, this common capacity goal cannot be practically

achieved in all the cases due to various EMC requirements. Except for the IPSD limit restrictions concerning human exposure to radio frequency electromagnetic fields [49], [50], other already licensed telecommunications services that surround overhead HV/BPL networks and operate at the same frequency range with overhead HV/BPL systems, demand their EMI protection.

- Nevertheless, the EMI protection of the communications systems that surround overhead HV/BPL networks can be fully achieved using suitable IPSD limits. These IPSD limits may be significantly more relaxed than those of today's EMI regulations. Since overhead HV/BPL networks are mainly located in remote or distant areas, the requirements for EMI protection in these zones remain very low due to the scarcity of close human and intense communications activities. Hence, there is the flexibility of allowing higher ad-hoc IPSD limits when there are no surrounding potential EMI victims. Consequently, depending on spatial and temporal EMI criteria, a more flexible EMI regulation approach, such as this of Figs. 10(a)-(d), is feasible taking under consideration only the ad-hoc EMI limits instead of using the universal fixed EMI regulations that are dramatically pessimistic in broadband performance terms.

- From different courses of their ECE program, ECE students have the opportunity to learn about MIMO technology advances. Recently, the concept of multiconductor diversity via introduction of MIMO/BPL technology makes its first but very promising and robust steps [39]-[43]. Overhead MIMO/HV/BPL technology permits a boost of the overall capacity, link reliability, diversity and range without additional bandwidth or transmit power when high IPSD regulations are adopted. New overhead MIMO/HV/BPL networks will permit a wide variety of more sophisticated SG applications such as real-time video surveillance/monitoring, diagnostics, distribution automation applications and real broadband internet connections to local surrounding communities to be introduced.

VI. Conclusions

This paper presents TEP method that is suitable for the study and the design of overhead HV/BPL networks from ECE students. In addition, TEP method demonstrates to undergraduate ECE students either the interaction between Microwave Engineering and Engineering Economics or the broadband potential of overhead HV/BPL networks when different overhead HV/BPL topologies, EMI regulations and noise conditions occur.

Based on the numerical results of techno-economic metrics such as end-to-end channel attenuation and capacity, major features of overhead HV/BPL networks have been reviewed for use in future transmission power grid networks and SG. In the light of information theory, the significant capacity performance of all considered overhead HV/BPL topologies is revealed. This broadband potential can further be enhanced by exploiting adaptive EMI regulations, the concept of scalable capacities, standardized topologies among different overhead and underground HV/BPL, MV/BPL and LV/BPL networks and topologies, wiser trade-offs among IPSD limits, noise, EMI protection and capacity thresholds, multi-hop BPL transmission, cooperative communications, and the integration of MIMO technology.

Especially, through the adoption of adaptive EMI regulations, which can be tuned according to noise conditions and other spatial and temporal EMI criteria, capacity

differences among different overhead HV/BPL topologies and noise conditions can efficiently be mitigated. This adaptive capacity mitigation technique offers significant results concerning the topic of scalable capacities among different overhead HV/BPL networks and sets an important step towards the design/operation of faster, more interoperable/intraoperable and more electromagnetic compatible BPL networks in the oncoming SG.

CONFLICTS OF INTEREST

The author declares that there is no conflict of interests regarding the publication of this paper.

REFERENCES

[1]   R. E. Collin, *Foundations for microwave engineering*, John Wiley & Sons, 2007.

[2]   D. M. Pozar, *Microwave Engineering*, Reading, MA, USA: Addison-Wesley Publishing Company, 1990.

[3]   L. T. Blank, A. J., Tarquin, and S. Iverson, *Engineering Economy*, New York, USA: McGraw-Hill, 2005.

[4]   G. E. Chatzarakis, S. N. Livieratos, and G. N. Miliaras, "An Integrated Method for Studying the Telegrapher's and Klein-Gordon Equations," *International Journal of Mathematical Education*, vol. 2, no. 2, pp. 83-98, 2012.

[5]   G. E. Chatzarakis, M. D. Tortoreli, and P. G. Cottis, "Teaching to undergraduates the optimum power transfer to a load under constraints," *IJEEE (International Journal of Electrical Engineering Education)*, vol. 41, no. 2, pp. 126-136, 2004. DOI: 10.7227/ijeee.41.2.4

[6]   R. Stoecker, "Evaluating and rethinking the case study," *The sociological review*, vol. 39, no.1, pp. 88-112, 1991. DOI: 10.1111/j.1467-954X.1991.tb02970.x

[7]   G. E. Chatzarakis, "Nodal Analysis Optimization Based on the Use of Virtual Current Sources: A Powerful New Pedagogical Method," *IEEE Transactions on Education*, vol. 52, no. 1, pp. 144-150, Feb. 2009. DOI: 10.1109/te.2008.921459

[8]   A. G. Lazaropoulos, "Review and progress towards the common broadband management of high-voltage transmission grids: model expansion and comparative modal analysis," *ISRN Electronics*, vol. 2012, Article ID 935286, pp. 1-18, 2012. DOI: 10.5402/2012/935286

[9]   A. G. Lazaropoulos, "Deployment concepts for overhead high voltage broadband over power lines connections with two-hop repeater system: Capacity countermeasures against aggravated topologies and high noise environments," *Progress in Electromagnetics Research B*, vol. 44, pp. 283-307, 2012. DOI: 10.2528/PIERB12081104

[10]   A. G. Lazaropoulos, "Broadband transmission characteristics of overhead high-voltage power line communication channels," *Progress in Electromagnetics Research B*, vol. 36, pp. 373-398, 2012. DOI: 10.2528/PIERB11091408

[11]   A. G. Lazaropoulos, "Broadband transmission and statistical performance properties of overhead high-voltage transmission networks," *Journal of Computer Networks and Commun.*, 2012, article ID 875632, 2012. DOI: 10.1155/2012/875632

[12]   A. G. Lazaropoulos, "Review and Progress towards the Capacity Boost of Overhead and Underground Medium-Voltage and Low-Voltage Broadband over Power Lines Networks: Cooperative Communications through Two- and Three-Hop Repeater Systems," _ISRN Electronics_, vol. 2013, Article ID 472190, pp. 1-19, 2013. DOI: 10.1155/2013/472190

[13]   A. G. Lazaropoulos and P. G. Cottis, "Transmission characteristics of overhead medium voltage power line communication channels," _IEEE Trans. Power Del._, vol. 24, no. 3, pp. 1164-1173, Jul. 2009. DOI: 10.1109/tpwrd.2008.2008467

[14]   A. G. Lazaropoulos and P. G. Cottis, "Broadband transmission via underground medium-voltage power lines-Part I: transmission characteristics," _IEEE Trans. Power Del._, vol. 25, no. 4, pp. 2414-2424, Oct. 2010. DOI: 10.1109/tpwrd.2010.2048929

[15]   A. G. Lazaropoulos and P. G. Cottis, "Capacity of overhead medium voltage power line communication channels," _IEEE Trans. Power Del._, vol. 25, no. 2, pp. 723-733, Apr. 2010. DOI: 10.1109/tpwrd.2009.2034907

[16]   A. G. Lazaropoulos and P. G. Cottis, "Broadband transmission via underground medium-voltage power lines-Part II: capacity," _IEEE Trans. Power Del._, vol. 25, no. 4, pp. 2425-2434, Oct. 2010. DOI: 10.1109/tpwrd.2010.2052113

[17]   T. Calliacoudas and F. Issa, "Multiconductor transmission lines and cables solver," An efficient simulation tool for plc channel networks development," presented at the _IEEE Int. Conf. Power Line Communications and Its Applications_, Athens, Greece, Mar. 2002.

[18]   N. Suljanović, A. Mujčić, M. Zajc, and J. F. Tasič, "Approximate computation of high-frequency characteristics for power line with horizontal disposition and middle-phase to ground coupling," _Electric Power Systems Research_, 69(1), 17-24. DOI: 10.1016/j.epsr.2003.07.005

[19]   M. Zajc, N. Suljanović, A. Mujčić, and J. F. Tasič, "Frequency characteristics measurement of overhead high-voltage power-line in low radio-frequency range," _IEEE Trans. Power Del._, vol. 22, no. 4, pp. 2142-2149, Oct. 2007. DOI: 10.1109/tpwrd.2007.905369

[20]   P. Amirshahi and M. Kavehrad, "High-frequency characteristics of overhead multiconductor power lines for broadband communications," _IEEE J. Sel. Areas Commun._, vol. 24, no. 7, pp. 1292-1303, Jul. 2006. DOI: 10.1109/jsac.2006.874399

[21]   M. D'Amore and M. S. Sarto, "A new formulation of lossy ground return parameters for transient analysis of multiconductor dissipative lines," _IEEE Trans. Power Del._, vol. 12, no. 1, pp. 303-314, Jan. 1997. DOI: 10.1109/61.568254

[22]   M. D'Amore and M. S. Sarto, "Simulation models of a dissipative transmission line above a lossy ground for a wide-frequency range-Part I: Single conductor configuration," _IEEE Trans. Electromagn. Compat._, vol. 38, no. 2, pp. 127-138, May 1996. DOI: 10.1109/15.494615

[23]   M. D'Amore and M. S. Sarto, "Simulation models of a dissipative transmission line above a lossy ground for a wide-frequency range-Part II: Multi-conductor configuration," _IEEE Trans. Electromagn. Compat._, vol. 38, no. 2, pp. 139-149, May 1996. DOI: 10.1109/15.494616

[24]   P. Amirshahi, "Broadband access and home networking through powerline networks," Ph.D. dissertation, Pennsylvania State Univ., University Park, PA, May 2006.

[25]   S. Galli and O. Logvinov, "Recent developments in the standardization of power line communications within the IEEE," _IEEE Commun. Mag._, vol. 46, no. 7, pp. 64-71, Jul. 2008. DOI: 10.1109/mcom.2008.4557044

[26]   D. Fenton and P. Brown, "Some aspects of benchmarking high frequency radiated emissions from wireline communications systems in the near and far fields," in _Proc. IEEE Int. Symp. on Power Line Communications and its Applications_, Malmö, Sweden, Apr. 2001, pp. 161-167.

[27]   M. Gebhardt, F. Weinmann, and K. Dostert, "Physical and regulatory constraints for communication over the power supply grid," _IEEE Commun. Mag._, vol. 41, no. 5, pp. 84-90, May 2003. DOI: 10.1109/mcom.2003.1200106

[28]   Ofcom, "Amperion PLT Measurements in Crieff," Ofcom, Tech. Rep., Sept. 2005.

[29]   NTIA, "Potential interference from broadband over power line (BPL) systems to federal government radio communications at 1.7-80 MHz Phase 1 Study Vol. 1," NTIA Rep. 04-413, Apr. 2004.

[30]   NATO, "HF Interference, Procedures and Tools (Interférences HF, procédures et outils) Final Report of NATO RTO Information Systems Technology," RTO-TR-ISTR-050, Jun. 2007.

[31]   FCC, "In the Matter of Amendment of Part 15 regarding new requirements and measurement guidelines for Access Broadband over Power Line Systems," FCC 04-245 Report and Order, Jul. 2008.

[32]   IEEE 1901 Working Group, "IEEE Standard for Broadband over Power Line Networks: Medium Access Control and Physical Layer Specifications," Tech. Report, 2010.

[33]   K. Youge, "HomePlug AV Technical Overview," in _Proc. IEEE Int. Symp. Power Line Communications and Its Applications_, Orlando, Florida, USA, Mar. 2006.

[34]   Ofcom, "DS2 PLT Measurements in Crieff," Ofcom, Tech. Rep. 793 (Part 2), May 2005.

[35]   Ofcom, "Ascom PLT Measurements in Winchester," Ofcom, Tech. Rep. 793 (Part 1), May 2005.

[36]   M. Götz, M. Rapp, and K. Dostert, "Power line channel characteristics and their effect on communication system design," _IEEE Commun. Mag._, vol. 42, no. 4, pp. 78-86, Apr. 2004. DOI: 10.1109/mcom.2004.1284933

[37]   R. Aquilué, I. Gutierrez, J. L. Pijoan, and G. Sánchez, "High-voltage multicarrier spread-spectrum system field test," _IEEE Trans. Power Del._, vol. 24, no. 3, pp. 1112-1121, Jul. 2009. DOI: 10.1109/tpwrd.2008.2002847

[38]   National Energy Technology Laboratory, "HV-BPL Phase 2, Field Test Report", Tech. Report, 2009.

[39]   T. Sartenaer and P. Delogne, "Deterministic modelling of the (Shielded) outdoor powerline channel based on the multiconductor transmission line equations," _IEEE J. Sel. Areas Commun._, vol. 24, no. 7, pp. 1277-1291, Jul. 2006. DOI: 10.1109/jsac.2006.874423

[40]   A. G. Lazaropoulos, "Green overhead and underground Multiple-Input Multiple-Output medium voltage broadband over power lines networks: Energy-efficient power control," _Journal of Global Optimization_, 57(3), 997-1024, 2013. DOI: 10.1007/s10898-012-9988-y.

[41]   A. G. Lazaropoulos, "Overhead and underground MIMO low voltage broadband over power lines networks and EMI regulations: Towards greener capacity

performances." *Computers & Electrical Engineering*, 39(7), 2214-2230, 2013. DOI: 10.1016/j.compeleceng.2013.02.003

[42] A. G. Lazaropoulos, "Broadband over Power Lines (BPL) Systems Convergence: Multiple-Input Multiple-Output (MIMO) Communications Analysis of Overhead and Underground Low-Voltage and Medium-Voltage BPL Networks," *ISRN Power Engineering*, vol. 2013, 30, 2013. DOI: 10.1155/2013/517940

[43] T. Sartenaer, "Multiuser communications over frequency selective wired channels and applications to the powerline access network" Ph.D. dissertation, Univ. Catholique Louvain, Louvain-la-Neuve, Belgium, Sep. 2004.

[44] C. R. Paul, *Analysis of Multiconductor Transmission Lines*. New York: Wiley, 1994.

[45] N. Suljanović, A. Mujčić, M. Zajc, and J. F. Tasič, "High-frequency characteristics of high-voltage power line," in *Proc. IEEE Int. Conf. on Computer as a Tool*, Ljubljana, Slovenia, Sep. 2003, pp. 310-314.

[46] M. Zimmermann and K. Dostert, "Analysis and modeling of impulsive noise in broad-band powerline communications," *IEEE Trans. Electromagn. Compat.*, vol. 44, no. 1, pp. 249-258, Feb. 2002. DOI: 10.1109/15.990732

[47] M. Katayama, T. Yamazato, and H. Okada, "A mathematical model of noise in narrowband power line communication systems," *IEEE J. Sel. Areas Commun.*, vol. 24, no. 7, pp. 1267-1276, Jul. 2006. DOI: 10.1109/jsac.2006.874408

[48] P. Amirshahi and M. Kavehrad, "Medium voltage overhead powerline broadband communications; Transmission capacity and electromagnetic interference," in *Proc. IEEE Int. Symp. Power Line Commun. Appl.*, Vancouver, BC, Canada, Apr. 2005, pp. 2-6.

[49] IEEE—International Committee on Electromagnetic Safety ICES, "Standard for safety levels with respect to human exposure to radio frequency electromagnetic fields, 3 kHz to 300 GHz," IEEE Std. C95.1-1991, 1992.

[50] International Commission on Non-Ionizing Radiation Protection, "Guidelines for limiting exposure to time-varying electric, magnetic, and electromagnetic fields (up to 300 GHz)," *Health Phys.*, vol. 74, no. 4, pp. 494–522, Apr. 1998.

A Review of Hydrothermal Carbonization of Carbohydrates for Carbon Spheres Preparation

Rui Li[1] and Abolghasem Shahbazi[2,*]

1: Joint School of Nanoscience and Nanoengineering, North Carolina A & T State University, Greensboro, NC, United States
2: Biological Engineering Program, Department of Natural Resources and Environmental Design, North Carolina A & T State University, 1601 East Market Street, Greensboro, NC 27411, United States

Carbon spheres have attracted a great deal of attention due to their applications as super capacitors, catalyst supports, and adsorbents. Carbon spheres can be prepared with controlled size and with oxygenated functional groups on the surface by the hydrothermal carbonization. The further processed products have a high surface area and high thermal stability. Among various methods for fabrication of carbon spheres, the hydrothermal carbonization is favored because of its mild operating conditions. In addition, hydrothermal carbonization can synthesize micro or nano scale carbon spheres environmentally friendly without employing organic solvents, surfactants, or catalysts. In this review, we present the effects of process parameters, structural characteristics of carbon spheres, possible formation mechanisms of carbon spheres, and applications in catalysis.

1. Introduction

1.1 Carbon Spheres Preparation and Hydrothermal Carbonization

Carbon spheres have received growing research attention due to their structure [1-3], high electrical conductivity [4], and excellent chemical stability [5, 6], which exhibit potential applications in supercapacitors [7, 8], catalyst supports [9], and adsorbents [10]. Various approaches have been used to prepare carbon spheres, such as chemical vapor deposition [11, 12], the templating method [13, 14], pyrolysis of carbon sources [15, 16], and hydrothermal treatment [17]. Among the aforementioned approaches, the hydrothermal treatment method is more favorable because of mild operational conditions [18] and the controllable size of carbon spheres [19, 20]. Thus, the hydrothermal carbonization method provides an efficient and scalable route to synthesize carbon particles at low pressure and low temperature [21].

Hydrothermal carbonization (HTC) is a thermochemical conversion process carried out under mild operating conditions in a sub-critical water medium [22], while the critical point occurs at 374°C and 22.1 MPa in water [23]. During the HTC procedure, the solution of carbohydrate precursors is usually heated to 130-250 °C under self-

generated pressures [17]. HTC has several advantages: Firstly, drying wet feedstocks is avoided, which opens up a large variety of feedstocks with a high water content of 75-90 wt% [24]. Secondly, HTC operates in water at low reaction temperature. Thirdly, the products generally exhibit uniform chemical and structural properties. However, the products have almost no porosity, unless they were synthesized in the presence of a template or subjected to additional heat treatment at a higher temperature [25].

1.2 History of Hydrothermal Carbonization

The application of hydrothermal carbonization for carbon formation was first reported by the German chemist Friedrich Bergius, who was awarded the Nobel Prize in 1913 [26]. Over a long period of time, the hydrothermal process was mainly focused on producing aqueous products such as phenol, furan derivatives, and organic acids. So, the residence time of hydrothermal treatment was shortened to prevent further aromatization or polymerization. Because of multiple applications of carbon spherical particles, a renaissance of HTC of carbohydrates to synthesize carbon spheres at a low temperature gradually came back since 2001. Especially, it had attracted the interest of many researchers after 2006, since Dr. Markus Antonietti at the Max Planck Institute of Colloids and Interfaces (Germany) investigated more details of HTC [25].

1.3 Materials and Methods

Table 1 summarizes hydrothermal carbonization studies for carbon spheres formation between 2001 and 2014. Until now, simple monosaccharide and oligosaccharides have been effectively employed as HTC starting materials [27]. Extensive studies have been carried out on glucose as a model compound. Spherical carbon particles were prepared through either a direct hydrothermal process or a hydrothermal process followed by a carbonization process [28]. Experiments were carried out in an autoclave partly filled with the precursor solution. The autoclave was heated to a specific temperature for a given period of time. The reaction temperature and pressure were below the critical point of water. The obtained solid products were separated by centrifugation and washed with water and ethanol to remove residual byproducts, like levulinic acid.

Table 1. Hydrothermal carbonization studies for carbon spheres formation in literature.

Products	Feedstock	Particle Size (μm)	HTC Conditions	Reference
Carbon nanospheres	Glucose	0.1-0.2	180°C for 4 h	[29]
Carbon spheres	Glucose	0.35	190°C for 4 h	[30]
Uniform carbon microspheres	Glucose, sucrose, and starch	0.4-6.0	170 to 240 °C	[31]
Carbon microspheres	Glucose	1-2	500°C for 12 h	[32]
Colloidal carbon spheres	Glucose	0.1-0.2	160°C for 6 h followed by 500°C for 4 h	[33]
Monodispersed hard carbon spheres	Sucrose	1-5	190°C for 5 h	[28]
Carbon microspheres	Starch	2	600°C for 12 h	[34]

2. Hydrothermal Carbonization Process

2.1 HTC Products of Glucose

The HTC products of glucose included an insoluble residue consisting of carbonaceous spherical particles, aqueous soluble products, and gaseous products [31]. The process water contained large quantities of aqueous soluble organic compounds [35]. Among them, a remarkable amount of hydroxymethylfurfural (HMF), levulinic acid, dihydroxyacetone, and formic acid were detected [20]. But phenol, phenol derivatives, other acids, and aldehydes were not found [36]. The gas phase consisted about 70-90% of CO_2, which derived from formate via decarboxylation [37]. Other gases were CO and H_2 [22].

Carbon spheres synthesized directly from carbohydrates at low temperatures possessed very low surface areas (<10 m^2/g) with a small volume of micropores, which was common for hydrothermal carbons [38]. Highly disordered carbon spheres from glucose were hydrophilic amorphous carbons [8, 31], which had a polymer-like structure consisting of polyfuranic chains [33]. This polymer-like structure was formed through polymerization or aromatization of furan-like molecules [36]. So, the core of carbon spheres was composed of hydrophobic polyfuran compounds [20]. Carbon spheres had carbonyl [27] and carboxylic acid functional groups on the hydrophilic surface [39].

As an efficient way to enhance surface area, heat treatment may remove the functional groups from the surface of HTC carbons, and create some micropores. The surface area of glucose-derived HTC carbons after further heat treatment at 1000°C could reach 400 m^2/g [28]. The morphology of HTC carbons did not change upon further heat treatment. But the surface appeared rougher because of micropore formation. If the heating temperature was too high, carbon spheres linked each other [40].

In terms of the carbon content, HTC of glucose increased the carbon content of colloid carbon spheres from 40 wt% to above 60 wt%, while the oxygen content was reduced [36]. After the further heat treatment, the carbon content increased from 60 wt% to above 80 wt%, while oxygen contents were correspondingly reduced [40].

2.2 Influence of Process Parameters

The size and the size distribution of colloidal carbon spheres prepared by HTC were influenced by processing temperature [41], reaction time, and the concentration of starting material [42].

2.2.1 Temperature

Colloidal carbon spheres were usually generated by HTC of glucose at a temperature of 170-260 °C. The minimum temperature for the hydrothermal carbon formation from glucose was 160°C, and hydrothermal carbonization did not take place below 160°C resulting in almost no solid residues [31]. At 180°C, HTC carbons formed were rich in carbonyl functionalities [41]. Increasing the HTC temperature led to hydrothermal carbons with a higher degree of aromatization, which was the normal tendency for a carbonization process. For example, hydrothermal carbon spheres, which were derived from HTC of 0.5 mol/L pure glucose solution for 4.5 h at different temperatures of 170, 180, 190, 210, and 230°C, had diameters of about 0.4, 0.44, 1.2, 1.2, 1.4 μm, respectively [31]. Above 280°C, only a very small fraction of carbon microspheres was generated, because the aliphatic carbon content decreased at temperatures higher than 260°C [43].

The processing temperature affected both the average diameter of carbonaceous particles and the size distribution. Higher temperature led to uniform particle diameter and a more homogeneous average size [41]. When the temperature was relatively low, glucose decomposed slowly. New nuclei may just form while the former nuclei already started carbonization, resulting in different growing time. So, under lower temperature, the size distribution was wider. When the temperature was relatively high, glucose can decompose completely very fast. All nuclei occurred at the same time, which led to a more homogeneous average size. But if the processing temperature was too high, formed microspheres had a risk to fuse together and become larger.

2.2.2 Residence Time

Exact residence time cannot be determined since reaction rates remained largely unknown, but typical published experimental residence time varied between 1 and 72 h [35]. A longer residence time led to higher reaction severity and less organic loss in the sugar solution. For instance, when HTC experiments were carried out at a constant concentration of 0.5 mol/L glucose and 160°C, as the residence time increased from 2 to 4, 6, 8, and 10 h, the diameters grew from 0.2 to 0.5, 0.8, 1.1, and 1.5 μm [42]. However, if the reaction time was too long, the produced carbon spheres fused, giving rise to particles with irregular shapes [30].

Dr. Titirici described in detail a conventional HTC process with a residence time [25]. When HTC experiments were carried out at a constant concentration of 10 wt% glucose and 180°C, during the first 2 h, no solid residues were observed, and glucose was dehydrated and decomposed into small soluble organic molecules. After 4 h, the color of the solution became dark orange suggesting that polymerization and aromatization occurred, called polymerization step. Past 5 h, the first solid precipitated out of the aqueous solution. After 8 h, a brown colloidal dispersion was formed. The black-brown solid formed spherically shaped particles of around 0.5 μm, aggregated together in 12 h. The growth process kept continuing, and the particle size increased to around 1.5 μm until all HMFs have been consumed.

2.2.3 Precursor Concentration

The size of carbon spheres increased with the elevated concentration of glucose solution within a certain concentration range [30]. When the concentration of glucose increased from 0.5 to 1 mol/L, the diameters grew from 1.2 to 1.4 μm, if HTC experiments were carried out at a constant temperature of 190ºC and dwell time of 4.5 h [31]. However, when the concentration reached to a certain degree, the size turned to be constant. For example, at same reaction conditions, when the concentration of sugar increased from 1.5 to 3.0 mol/L, the average diameters in two samples were all 5 μm [28]. In addition, excessive concentration led to a larger particle size distribution. On one hand, a high concentration of carbon microspheres increased the probability of crosslinking. On the other hand, a higher concentration of glucose needed a longer time to dehydrate completely, which led to different formation time.

2.2.4 Carbohydrate Precursors

HTC had a wide range of possible sources such as carbohydrates (glucose, fructose, xylose, sucrose, cellulose, and starch) [31, 34], biomass [35], sewage sludge, animal manure, municipal solid waste [44], agricultural residues, and algae [24]. It's difficult for HTC of biomass to form carbon spheres with regular morphology in a

uniform chemical structure compared to simple saccharides. For example, hydrothermal carbonization of eucalyptus sawdust or barley straw at 250°C formed carbon microspheres with the size of 1-10 μm from cellulose fraction of biomass. But these carbon microspheres covered with particles retained the cellular appearance of raw materials [45]. Therefore, carbon spheres from HTC of biomass were rarely used in catalytic and electrode applications. So far, carbohydrates have been ideal starting materials for preparing carbon spheres, because they were cheap and favored in the dehydration process [46], and products had a uniform chemical structure. All materials obtained from hexoses-based mono- (glucose, HMF), di- (maltose, sucrose), and polysaccharides (amylopectin, starch) can be hydrolyzed to glucose units. Under similar operational conditions, the diameters of carbon microspheres depended on the type of saccharides used. The average diameter of carbon microspheres derived from different carbohydrates had a sequence of sucrose > starch > glucose [31]. This variation was related to the number of decomposed species generated from different saccharides, which were obviously greater in the case of starch and sucrose due to their polysaccharide and disaccharide nature, respectively [31]. Carbonaceous materials derived from pentose-based carbohydrates showed morphological and chemical differences from hexose-based ones [27]. Because furfural was the main dehydration product from pentose-based saccharides, while HMF was the main dehydration product from hexoses-based saccharides [40].

2.2.5 pH

The formation of acids was inevitable during the HTC, lowering the pH value to ~3 [31]. This acidic condition tended to increase the reaction rate in HTC, because the hydronium ions generated from these acids catalyzed dehydration and further polymerization of HMF [25]. A pH of 1.5 solution could increase glucose destruction [47]. The addition of acid in the fructose solution caused high yields of HMF and furfural, and decreased yields of pyruvaldehyde and lactic acid [48].

2.2.6 Pressure

Pressure had no significant effect on promoting HTC conversion, because the HTC reaction occurred in the liquid phase. The resulting pressure in a close compartment was higher than the saturated vapor pressure due to the formation of gases.

2.3 Possible HTC Mechanism of Glucose and Cellulose

The possible mechanism is schematically illustrated in Fig. 1. When glucose was dissolved in water, it existed in three forms: an open chain, a pyranose ring, and a furanose ring [49]. The levoglucosan (1, 6-anhydro-β-D-glucopyranose) was produced by the dehydration of glucose. Erythrose and glycolaldehyde were transformed from glucose by retro-aldol condensation [50]. Glyceraldehyde was transformed from fructose, isomerization of glucose, by retro-aldol condensation [51]. Dihydroxyacetone was produced through reversible isomerization of glyceraldehydes, while both dehydrated to form pyruvaldehyde [52]. Lactic acid was formed from pyruvaldehyde by benzilic acid rearrangement [53]. Hydroxymethylfurfural (HMF) was produced from dehydration of glucose [54, 55], and HMF hydrolysis produced levulinic acid and formic acid [56]. 1, 2, 4-benzenetriol was a decomposition product of HMF [57], while the 1, 2, 4-benzenetriol could continue to polymerize with HMF or other intermediates [58].

Polymerization and condensation reactions may be induced by intermolecular dehydration or aldol condensation, forming soluble polymers [59]. At the same time, the aromatization of polymers took place. Aromatic clusters may be produced by the intermolecular dehydration of aromatized molecules generated in the decomposition or dehydration. The presence of reactive aldehyde and alcohol groups in HMF suggested that this compound may easily polymerize to give long-chain molecules [60]. HMF was also in situ "polymerized" to polymeric carbonaceous materials [61].

The growth of nucleated carbon particles may follow the LaMer model [62]. When the concentration of soluble polymers reached the critical supersaturation point, nucleation occurred upon segregating the formed polymer that was phased out of the aqueous solution. Then the nuclei grew outwards by diffusion of solutes present in the solution towards their surface. These species were linked to the surface of microspheres via reactive oxygen-containing functional groups [41]. This process was called carbonization [31]. When the growth stopped, carbon materials formed from glucose had a condensed furanic system consisting of a hydrophobic core and a hydrophilic shell embedded with levulinic acid [30].

During HTC of cellulose, most cellulosic substrates underwent intramolecular condensation, dehydration, and decarboxylation reactions; and were converted to aromatic network structures. A very limited degree of hydrolysis and consequential individual glucose formation most likely took place simultaneously at the cellulose-water interface [41], and then reactions followed the same reaction pathway as glucose during the hydrothermal treatment [31].
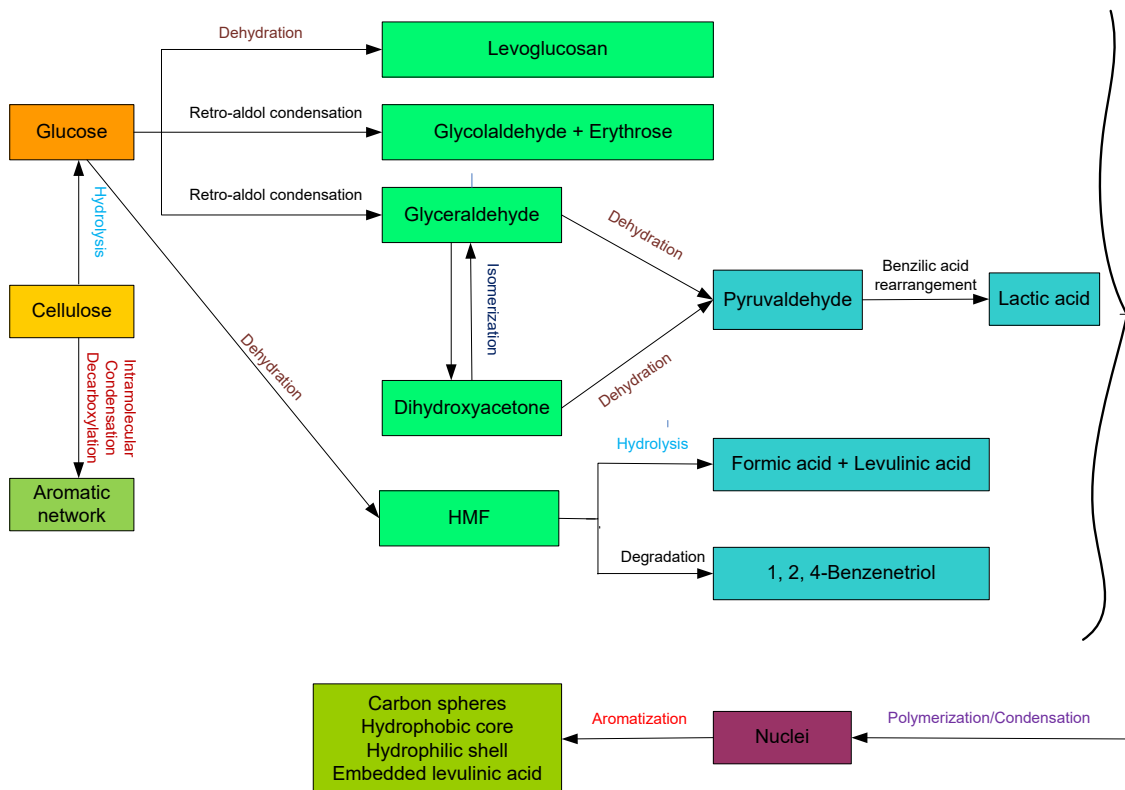
Figure 1. Schematic formation model for carbon spheres obtained from glucose and cellulose.

2.4 Applications of Hydrothermal Carbons

Carbon materials derived from HTC processes have been used as absorbents for removal of Cr(VI) [63] and Pb(II) ions in water [10], and materials for lithium-ion batteries [64-67]. Due to the good dispersion and functional groups prepared by the HTC method, carbon spheres can be ideal catalyst supports [68, 69].

One step HTC of the carbohydrate and metal solution can synthesize core-shell structure carbon spheres with hydrophobic metals as core and carbon as a shell. Silver cored carbon spheres were synthesized by HTC of $HAuCl_4$ and glucose at 160-180 °C for 4-20 h [42]. Carbon spheres embedded with iron oxide nanoparticles, an excellent catalyst in the Fischer-Tropsch synthesis, was synthesized by HTC of glucose and iron nitrate [68]. During the hydrothermal treatment, iron nitrate was transformed to FeOOH, which was further reduced to iron oxide by hydrogen during the carbonization process. Carbon spheres embedded with palladium nanoparticles were synthesized by HTC of furfural and palladium acetylacetonate. During the HTC process, the palladium acetylacetonate was reduced to elemental metallic palladium nanoparticles [70].

Metal oxides hollow spheres could be synthesized in a one-pot synthesis via HTC of carbohydrate and metal salt. During this HTC process, a hydrophilic shell with -OH or C=O groups were prepared, and metal ions incorporated into the hydrophilic shell of carbon spheres. Hollow metal oxide spheres were obtained by calcining in air to remove encapsulated carbon. For example, the TiO_2-hollow spheres were synthesized using carbon spheres as a template. Carbon spheres have -OH groups on their surface. The titanium source incorporated into the hydrophilic shell through the covalent –O-Ti bonding [71].

Inversely, carbon spheres with hollow structures can be made using metal as sacrificial templates. First, carbon spheres with the metal inside were made from hydrothermally treated carbohydrate and metal mixture. Then, the removal of metal resulted in hollow carbon spheres. For example, hollow carbon spheres were prepared from the HTC of glucose and Zn particles at 550°C for 8 h. The products were washed with HCl to remove Zn and ZnO inside. The hollow carbon spheres were about 1-2 μm in diameter, and the surface area was 207 m^2/g [72].

3. CONCLUSIONS

Hydrothermal carbonization (HTC) of carbohydrates is shown as a green and sustainable technology to synthesize carbon micro or nano spheres, which have a core-shell structure with a highly hydrophobic and aromatic nucleus, and a hydrophilic shell containing oxygenated functional groups. HTC reactions take place in pure water at mild conditions with cheap precursors. The size and the size distribution of carbon spheres could be modulated by synthesis conditions such as the treatment temperature, the reaction time, the concentration of starting materials, and the type of precursors. Detailed mechanisms involved in HTC of glucose include hydrolysis, dehydration, polymerization, condensation, and aromatization. Although the mechanism of glucose HTC is almost confirmed, the mechanism for real biomass conversion is still under investigation, because of unknown contributions from lignin, protein, and lipid. The model is needed to predict the particle size and the size distribution from parameters such as temperature, residue time, precursor concentration, different saccharides, and solution filing degree. The new applications of carbon spheres are still being investigated.

ACKNOWLEDGMENTS

CONFLICTS OF INTEREST

The authors declare that there is no conflict of interests regarding the publication of this paper.

REFERENCES

[1]   Mi, C., and Chen, W. (2014). Highly nanoporous carbon microflakes from discarded dental impression materials. *Materials Letters*, 114, 129-131. DOI: 10.1016/j.matlet.2013.10.010

[2]   White, R. J. (2015). *Porous Carbon Materials from Sustainable Precursors*, Royal Society of Chemistry

[3]   Chen, J., Lang, Z., Xu, Q., Hu, B., Fu, J., Chen, Z., and Zhang, J. (2013). Facile Preparation of monodisperse carbon spheres: Template-free construction and their hydrogen storage properties. *ACS Sustainable Chemistry & Engineering*, 1(8), 1063-1068. DOI: 10.1021/sc400124b

[4]   Zhang, K., Zhao, Q., Tao, Z., and Chen, J. (2013). Composite of sulfur impregnated in porous hollow carbon spheres as the cathode of Li-S batteries with high performance. *Nano Research*, 6(1), 38-46. DOI: 10.1007/s12274-012-0279-1

[5]   Zhang, Z., Xiao, F., Xi, J., Sun, T., Xiao, S., Wang, H., Wang, S., and Liu, Y. (2014). Encapsulating Pd Nanoparticles in Double-Shelled Graphene@Carbon Hollow Spheres for Excellent Chemical Catalytic Property. *Scientific reports*, 4, Article number: 4053. DOI: 10.1038/srep04053

[6]   Alazemi, A. A., Etacheri, V., Dysart, A., Stacke, L.-E., Pol, V., and Sadeghi, F. (2015). Ultrasmooth Submicron Carbon Spheres as Lubricant Additives for Friction and Wear Reduction. *ACS Applied Materials & Interfaces*, 7(9), 5514–5521. DOI: 10.1021/acsami.5b00099

[7]   Tien, B., Xu, M., and Liu, J. (2010). Synthesis and electrochemical characterization of carbon spheres as anode material for lithium-ion battery. *Materials Letters*, 64(13), 1465-1467. DOI: 10.1016/j.matlet.2010.03.061

[8]   Tooming, T., Thomberg, T., Romann, T., Palm, R., Jänes, A., and Lust, E. (2013). Carbon materials for supercapacitor application by hydrothermal carbonization of D-glucose. *IOP Conf. Ser.: Mater. Sci. Eng*, 49, 012020. DOI: 10.1088/1757-899X/49/1/012020

[9]   Auer, E., Freund, A., Pietsch, J., and Tacke, T. (1998). Carbons as supports for industrial precious metal catalysts. *Applied Catalysis A: General*, 173(2), 259-271. DOI: 10.1016/S0926-860X(98)00184-7

[10]   Chen, L.-F., Liang, H.-W., Lu, Y., Cui, C.-H., and Yu, S.-H. (2011). Synthesis of an Attapulgite Clay@Carbon Nanocomposite Adsorbent by a Hydrothermal

Carbonization Process and Their Application in the Removal of Toxic Metal Ions from Water. *Langmuir*, 27(14), 8998-9004. DOI: 10.1021/la2017165

[11]   Qian, H.-s., Han, F.-m., Zhang, B., Guo, Y.-c., Yue, J., and Peng, B.-x. (2004). Non-catalytic CVD preparation of carbon spheres with a specific size. *Carbon*, 42(4), 761-766. DOI: 10.1016/j.carbon.2004.01.004

[12]   Serp, P., Feurer, R., Kalck, P., Kihn, Y., Faria, J., and Figueiredo, J. (2001). A chemical vapour deposition process for the production of carbon nanospheres. *Carbon*, 39(4), 621-626. DOI: 10.1016/S0008-6223(00)00324-9

[13]   Joo, J. B., Kim, P., Kim, W., Kim, J., Kim, N. D., and Yi, J. (2008). Simple preparation of hollow carbon sphere via templating method. *Current Applied Physics*, 8(6), 814-817. DOI: 10.1016/j.cap.2007.04.038

[14]   Ryoo, R., Joo, S. H., and Jun, S. (1999). Synthesis of Highly Ordered Carbon Molecular Sieves via Template-Mediated Structural Transformation. *The Journal of Physical Chemistry B*, 103(37), 7743-7746. DOI: 10.1021/jp991673a

[15]   Jin, Y. Z., Gao, C., Hsu, W. K., Zhu, Y., Huczko, A., Bystrzejewski, M., Roe, M., Lee, C. Y., Acquah, S., and Kroto, H. (2005). Large-scale synthesis and characterization of carbon spheres prepared by direct pyrolysis of hydrocarbons. *Carbon*, 43(9), 1944-1953. DOI: 10.1016/j.carbon.2005.03.002

[16]   Friedel, B., and Greulich-Weber, S. (2006). Preparation of Monodisperse, Submicrometer Carbon Spheres by Pyrolysis of Melamine–Formaldehyde Resin. *small*, 2(7), 859-863. DOI: 10.1002/smll.200500516

[17]   Titirici, M.-M., and Antonietti, M. (2010). Chemistry and materials options of sustainable carbon materials made by hydrothermal carbonization. *Chemical Society Reviews*, 39(1), 103-116. DOI: 10.1039/B819318P

[18]   Byrappa, K., and Adschiri, T. (2007). Hydrothermal technology for nanotechnology. *Progress in Crystal Growth and Characterization of Materials*, 53(2), 117-166. DOI: 10.1016/j.pcrysgrow.2007.04.001

[19]   Yao, C., Shin, Y., Wang, L.-Q., Windisch, C. F., Samuels, W. D., Arey, B. W., Wang, C., Risen, W. M., and Exarhos, G. J. (2007). Hydrothermal Dehydration of Aqueous Fructose Solutions in a Closed System. *The Journal of Physical Chemistry C*, 111(42), 15141-15145. DOI: 10.1021/jp074188l

[20]   Baccile, N., Laurent, G., Babonneau, F., Fayon, F., Titirici, M.-M., and Antonietti, M. (2009). Structural Characterization of Hydrothermal Carbon Spheres by Advanced Solid-State MAS 13C NMR Investigations. *The Journal of Physical Chemistry C*, 113(22), 9644-9654. DOI: 10.1021/jp901582x

[21]   Krishnamurthy, G., and Namitha, R. (2013). Synthesis of structurally novel carbon micro/nanospheres by low temperature-hydrothermal process. *Journal of the Chilean Chemical Society*, 58(3), 1930-1933. DOI: 10.4067/S0717-97072013000300030

[22]   Ramke, H.-G., Blöhse, D., Lehmann, H.-J., and Fettig, J. (2009). Hydrothermal carbonization of organic waste. In: *Proc., Twelfth International Waste Management and Landfill Symposium*, Sardinia, Italy.

[23]   Bröll, D., Kaul, C., Kraemer, A., Krammer, P., Richter, T., Jung, M., Vogel, H., and Zehner, P. (1999). Chemistry in Supercritical Water. *Angewandte Chemie International Edition*, 38(20), 2998-3014. DOI: 10.1002/(SICI)1521-3773(19991018)38:20<2998::AID-ANIE2998>3.0.CO;2-L

[24]   Libra, J. A., Ro, K. S., Kammann, C., Funke, A., Berge, N. D., Neubauer, Y., Titirici, M.-M., Fühner, C., Bens, O., and Kern, J. (2011). Hydrothermal

carbonization of biomass residuals: a comparative review of the chemistry, processes and applications of wet and dry pyrolysis. *Biofuels*, 2(1), 71-106. DOI: 10.4155/BFS.10.81

[25]   Titirici, M.-M. (2013). *Sustainable carbon materials from hydrothermal processes*, Wiley Online Library.

[26]   Stranges, A. N. (1984). Friedrich Bergius and the Rise of the German Synthetic Fuel Industry. *Isis*, 75(4), 643-667. DOI: 10.2307/232411

[27]   Titirici, M.-M., Antonietti, M., and Baccile, N. (2008). Hydrothermal carbon from biomass: a comparison of the local structure from poly-to monosaccharides and pentoses/hexoses. *Green Chemistry*, 10(11), 1204-1212. DOI: 10.1039/B807009A

[28]   Wang, Q., Li, H., Chen, L., and Huang, X. (2001). Monodispersed hard carbon spherules with uniform nanopores. *Carbon*, 39(14), 2211-2214. DOI: 10.1016/S0008-6223(01)00040-9

[29]   Qi, X., Lian, Y., Yan, L., and Smith, R. L. (2014). One-step preparation of carbonaceous solid acid catalysts by hydrothermal carbonization of glucose for cellulose hydrolysis. *Catalysis Communications*, 57, 50-54. DOI: 10.1016/j.catcom.2014.07.035

[30]   Li, M., Li, W., and Liu, S. (2011). Hydrothermal synthesis, characterization, and KOH activation of carbon spheres from glucose. *Carbohydrate Research*, 346(8), 999-1004. DOI: 10.1016/j.carres.2011.03.020

[31]   Sevilla, M., and Fuertes, A. B. (2009). Chemical and structural properties of carbonaceous products obtained by hydrothermal carbonization of saccharides. *Chemistry-A European Journal*, 15(16), 4195-4203. DOI: 10.1002/chem.200802097

[32]   Mi, Y., Hu, W., Dan, Y., and Liu, Y. (2008). Synthesis of carbon micro-spheres by a glucose hydrothermal method. *Materials Letters*, 62(8), 1194-1196. DOI: 10.1016/j.matlet.2007.08.011

[33]   Yi, Z., Liang, Y., Lei, X., Wang, C., and Sun, J. (2007). Low-temperature synthesis of nanosized disordered carbon spheres as an anode material for lithium ion batteries. *Materials Letters*, 61(19), 4199-4203. DOI: 10.1016/j.matlet.2007.01.054

[34]   Zheng, M., Liu, Y., Xiao, Y., Zhu, Y., Guan, Q., Yuan, D., and Zhang, J. (2009). An easy catalyst-free hydrothermal method to prepare monodisperse carbon microspheres on a large scale. *The Journal of Physical Chemistry C*, 113(19), 8455-8459. DOI: 10.1021/jp811356a

[35]   Funke, A., and Ziegler, F. (2010). Hydrothermal carbonization of biomass: a summary and discussion of chemical mechanisms for process engineering. *Biofuels, Bioproducts and Biorefining*, 4(2), 160-177. DOI: 10.1002/bbb.198

[36]   Aydıncak, K., Yumak, T. r., Sınağ, A., and Esen, B. (2012). Synthesis and Characterization of Carbonaceous Materials from Saccharides (Glucose and Lactose) and Two Waste Biomasses by Hydrothermal Carbonization. *Industrial & Engineering Chemistry Research*, 51(26), 9145-9152. DOI: 10.1021/ie301236h

[37]   Robbiani, Z. (2013). Hydrothermal carbonization of biowaste/fecal sludge: Conception and construction of a HTC prototype research unit for developing countries. Master's Thesis, Swiss Federal Institute of Technology in Zurich (ETHZ).

[38]   Demir-Cakan, R., Baccile, N., Antonietti, M., and Titirici, M.-M. (2009). Carboxylate-Rich Carbonaceous Materials via One-Step Hydrothermal

Carbonization of Glucose in the Presence of Acrylic Acid. *Chemistry of materials*, 21(3), 484-490. DOI: 10.1021/cm802141h

[39]   Demir-Cakan, R., Hu, Y.-S., Antonietti, M., Maier, J., and Titirici, M.-M. (2008). Facile One-Pot Synthesis of Mesoporous SnO2 Microspheres via Nanoparticles Assembly and Lithium Storage Properties. *Chemistry of materials*, 20(4), 1227-1229. DOI: 10.1021/cm7031288

[40]   Yu, L., Falco, C., Weber, J., White, R. J., Howe, J. Y., and Titirici, M.-M. (2012). Carbohydrate-Derived Hydrothermal Carbons: A Thorough Characterization Study. *Langmuir*, 28(33), 12373-12383. DOI: 10.1021/la3024277

[41]   Falco, C., Baccile, N., and Titirici, M.-M. (2011). Morphological and structural differences between glucose, cellulose and lignocellulosic biomass derived hydrothermal carbons. *Green Chemistry*, 13(11), 3273-3281. DOI: 10.1039/C1GC15742F

[42]   Sun, X., and Li, Y. (2004). Colloidal Carbon Spheres and Their Core/Shell Structures with Noble-Metal Nanoparticles. *Angewandte Chemie International Edition*, 43(5), 597-601. DOI: 10.1002/anie.200352386

[43]   Yin, S., and Tan, Z. (2012). Hydrothermal liquefaction of cellulose to bio-oil under acidic, neutral and alkaline conditions. *Applied Energy*, 92, 234-239. DOI: 10.1016/j.apenergy.2011.10.041

[44]   Berge, N. D., Ro, K. S., Mao, J., Flora, J. R. V., Chappell, M. A., and Bae, S. (2011). Hydrothermal Carbonization of Municipal Waste Streams. *Environmental Science & Technology*, 45(13), 5696-5703. DOI: 10.1021/es2004528

[45]   Sevilla, M., Maciá-Agulló, J. A., and Fuertes, A. B. (2011). Hydrothermal carbonization of biomass as a route for the sequestration of CO2: Chemical and structural properties of the carbonized products. *Biomass and Bioenergy*, 35(7), 3152-3159. DOI: 10.1016/j.biombioe.2011.04.032

[46]   Chheda, J. N., Román-Leshkov, Y., and Dumesic, J. A. (2007). Production of 5-hydroxymethylfurfural and furfural by dehydration of biomass-derived mono-and poly-saccharides. *Green Chemistry*, 9(4), 342-350. DOI: 10.1039/B611568C

[47]   Xiang, Q., Lee, Y., and Torget, R. (2004). Kinetics of glucose decomposition during dilute-acid hydrolysis of lignocellulosic biomass. *Applied Biochemistry and Biotechnology*, 115(1-3), 1127-1138. DOI: 10.1385/abab:115:1-3:1127

[48]   Antal, M. J., Mok, W. S., and Richards, G. N. (1990). Mechanism of formation of 5-(hydroxymethyl)-2-furaldehyde from D-fructose and sucrose. *Carbohydrate Research*, 199(1), 91-109. DOI: 10.1016/0008-6215(90)84096-D

[49]   Peterson, A. A., Vogel, F., Lachance, R. P., Fröling, M., Antal Jr, M. J., and Tester, J. W. (2008). Thermochemical biofuel production in hydrothermal media: A review of sub-and supercritical water technologies. *Energy & Environmental Science*, 1(1), 32-65. DOI: 10.1039/B810100K

[50]   Sasaki, M., Goto, K., Tajima, K., Adschiri, T., and Arai, K. (2002). Rapid and selective retro-aldol condensation of glucose to glycolaldehyde in supercritical water. *Green Chemistry*, 4(3), 285-287. DOI: 10.1039/b203968k

[51]   Srokol, Z., Bouche, A.-G., van Estrik, A., Strik, R. C., Maschmeyer, T., and Peters, J. A. (2004). Hydrothermal upgrading of biomass to biofuel; studies on some monosaccharide model compounds. *Carbohydrate Research*, 339(10), 1717-1726. DOI: 10.1016/j.carres.2004.04.018

[52]   Kabyemela, B. M., Adschiri, T., Malaluan, R., and Arai, K. (1997). Degradation Kinetics of Dihydroxyacetone and Glyceraldehyde in Subcritical and Supercritical

Water. *Industrial & Engineering Chemistry Research*, 36(6), 2025-2030. DOI: 10.1021/ie960747r

[53]   Chen, L. (2011). Conversion of Glycerol to Lactic Acid under Low Corrosive Conditions with Homogeneous and Heterogeneous Catalysts. Master's Thesis, University of Tennessee

[54]   Asghari, F. S., and Yoshida, H. (2007). Kinetics of the Decomposition of Fructose Catalyzed by Hydrochloric Acid in Subcritical Water: Formation of 5-Hydroxymethylfurfural, Levulinic, and Formic Acids. *Industrial & Engineering Chemistry Research*, 46(23), 7703-7710. DOI: 10.1021/ie061673e

[55]   Möller, M., Nilges, P., Harnisch, F., and Schröder, U. (2011). Subcritical Water as Reaction Environment: Fundamentals of Hydrothermal Biomass Transformation. *ChemSusChem*, 4(5), 566-579. DOI: 10.1002/cssc.201000341

[56]   Weingarten, R., Conner, W. C., and Huber, G. W. (2012). Production of levulinic acid from cellulose by hydrothermal decomposition combined with aqueous phase dehydration with a solid acid catalyst. *Energy & Environmental Science*, 5(6), 7559-7574. DOI: 10.1039/c2ee21593d

[57]   Luijkx, G. C. A., van Rantwijk, F., and van Bekkum, H. (1993). Hydrothermal formation of 1,2,4-benzenetriol from 5-hydroxymethyl-2-furaldehyde and d-fructose. *Carbohydrate Research*, 242(0), 131-139. DOI: 10.1016/0008-6215(93)80027-C

[58]   Chuntanapum, A., and Matsumura, Y. (2009). Formation of Tarry Material from 5-HMF in Subcritical and Supercritical Water. *Industrial & Engineering Chemistry Research*, 48(22), 9837-9846. DOI: 10.1021/ie900423g

[59]   Salak Asghari, F., and Yoshida, H. (2006). Acid-Catalyzed Production of 5-Hydroxymethyl Furfural from d-Fructose in Subcritical Water. *Industrial & Engineering Chemistry Research*, 45(7), 2163-2173. DOI: 10.1021/ie051088y

[60]   Scallet, B. L., and Gardner, J. H. (1945). Formation of 5-Hydroxymethylfurfural from D-Glucose in Aqueous Solution. *Journal of the American Chemical Society*, 67(11), 1934-1935. DOI: 10.1021/ja01227a017

[61]   Patil, S. K., and Lund, C. R. (2011). Formation and growth of humins via aldol addition and condensation during acid-catalyzed conversion of 5-hydroxymethylfurfural. *Energy & Fuels*, 25(10), 4745-4755. DOI: 10.1021/ef2010157

[62]   LaMer, V. K., and Dinegar, R. H. (1950). Theory, production and mechanism of formation of monodispersed hydrosols. *Journal of the American Chemical Society*, 72(11), 4847-4854. DOI: 10.1021/ja01167a001

[63]   Li, T., Shen, J., Huang, S., Li, N., and Ye, M. (2014). Hydrothermal carbonization synthesis of a novel montmorillonite supported carbon nanosphere adsorbent for removal of Cr (VI) from waste water. *Applied Clay Science*, 93–94, 48-55. DOI: 10.1016/j.clay.2014.02.015

[64]   Yang, R., Zhao, W., Zheng, J., Zhang, X., and Li, X. (2010). One-Step Synthesis of Carbon-Coated Tin Dioxide Nanoparticles for High Lithium Storage. *The Journal of Physical Chemistry C*, 114(47), 20272-20276. DOI: 10.1021/jp107396a

[65]   Zhao, N., Wu, S., He, C., Wang, Z., Shi, C., Liu, E., and Li, J. (2013). One-pot synthesis of uniform Fe3O4 nanocrystals encapsulated in interconnected carbon nanospheres for superior lithium storage capability. *Carbon*, 57, 130-138. DOI: 10.1016/j.carbon.2013.01.056

[66]   Lou, X. W., Chen, J. S., Chen, P., and Archer, L. A. (2009). One-Pot Synthesis of Carbon-Coated SnO2 Nanocolloids with Improved Reversible Lithium Storage Properties. *Chemistry of materials*, 21(13), 2868-2874. DOI: 10.1021/cm900613d

[67]   Chen, J. S., Zhang, Y., and Lou, X. W. (2011). One-Pot Synthesis of Uniform Fe3O4 Nanospheres with Carbon Matrix Support for Improved Lithium Storage Capabilities. *ACS Applied Materials & Interfaces*, 3(9), 3276-3279. DOI: 10.1021/am201079z

[68]   Yu, G., Sun, B., Pei, Y., Xie, S., Yan, S., Qiao, M., Fan, K., Zhang, X., and Zong, B. (2009). FexOy@C Spheres as an Excellent Catalyst for Fischer−Tropsch Synthesis. *Journal of the American Chemical Society*, 132(3), 935-937. DOI: 10.1021/ja906370b

[69]   Cheng, J., Wang, Y., Teng, C., Shang, Y., Ren, L., and Jiang, B. (2014). Preparation and characterization of monodisperse, micrometer-sized, hierarchically porous carbon spheres as catalyst support. *Chemical Engineering Journal*, 242, 285-293. DOI: 10.1016/j.cej.2013.12.089

[70]   Makowski, P., Cakan, R. D., Antonietti, M., Goettmann, F., and Titirici, M.-M. (2008). Selective partial hydrogenation of hydroxy aromatic derivatives with palladium nanoparticles supported on hydrophilic carbon. *Chemical Communications*(8), 999-1001. DOI: 10.1039/B717928F

[71]   Shen, W., Zhu, Y., Dong, X., Gu, J., and Shi, J. (2005). A new strategy to synthesize TiO2-hollow spheres using carbon spheres as template. *ChemInform*, 34(40), no. DOI: 10.1002/chin.200540213

[72]   Wang, F.-L., Pang, L.-L., Jiang, Y.-Y., Chen, B., Lin, D., Lun, N., Zhu, H.-L., Liu, R., Meng, X.-L., and Wang, Y. (2009). Simple synthesis of hollow carbon spheres from glucose. *Materials Letters*, 63(29), 2564-2566. DOI: 10.1016/j.matlet.2009.09.008

To cite this article:

Li, R. and Shahbazi, A. (2015). "A Review of Hydrothermal Carbonization of Carbohydrates for Carbon Spheres Preparation." *Trends in Renewable Energy*, 1(1), 43-56. http://dx.doi.org/10.17737/tre.2015.1.1.009